

THE MINISTRY OF SCIENCE AND HIGHER EDUCATION OF THE RUSSIAN FEDERATION



ISSN 2687-0517

Computing, Telecommunications and Control

**Vol. 17, No. 2
2024**

Peter the Great St. Petersburg
Polytechnic University
2024

COMPUTING, TELECOMMUNICATIONS AND CONTROL

EDITORIAL COUNCIL

Prof. Dr. *Rafael M. Yusupov* corresponding member of RAS, St. Petersburg Institute for Informatics and Automation of the RAS, Russia,
Prof. Dr. *Dmitry G. Arseniev* corresponding member of RAS, Peter the Great St. Petersburg Polytechnic University, Russia,
Prof. Dr. *Vladimir V. Voevodin* corresponding member of RAS, Lomonosov Moscow State University, Russia,
Prof. Dr. *Vladimir S. Zaborovsky*, Peter the Great St. Petersburg Polytechnic University, Russia,
Prof. Dr. *Vladimir N. Kozlov*, Peter the Great St. Petersburg Polytechnic University, Russia,
Prof. Dr. *Alexandr E. Fotiadi*, Peter the Great St. Petersburg Polytechnic University, Russia,
Prof. Dr. *Igor G. Chernorutsky*, Peter the Great St. Petersburg Polytechnic University, Russia.

EDITORIAL BOARD

Editor-in-chief

Prof. Dr. *Alexander S. Korotkov*, Peter the Great St. Petersburg Polytechnic University, Russia;

Members:

Assoc. Prof. Dr. *Pavel D. Drobintsev*, Peter the Great St. Petersburg Polytechnic University, Russia;
Assoc. Prof. Dr. *Vladimir M. Itsyson*, Peter the Great St. Petersburg Polytechnic University, Russia;
Prof. Dr. *Philippe Ferrari*, Grenoble Alpes University, France;
Prof. Dr. *Yevgeni Koucheryavy*, Tampere University of Technology, Finland;
Prof. Dr. *Wolfgang Krautschneider*, Hamburg University of Technology, Germany;
Prof. Dr. *Fa-Long Luo*, University of Washington, USA;
Prof. Dr. *Sergey B. Makarov*, Peter the Great St. Petersburg Polytechnic University, Russia;
Prof. Dr. *Emil Novakov*, Grenoble Alpes University, France;
Prof. Dr. *Nikolay N. Prokopenko*, Don State Technical University, Russia;
Prof. Dr. *Mikhail G. Putrya*, National Research University of Electronic Technology, Russia;
Sen. Assoc. Prof. Dr. *Evgeny Pyshkin*, University of Aizu, Japan;
Prof. Dr. *Viacheslav P. Shkodyrev*, Peter the Great St. Petersburg Polytechnic University, Russia;
Prof. Dr. *Vladimir A. Sorotsky*, Peter the Great St. Petersburg Polytechnic University, Russia
Prof. Dr. *Peter V. Trifonov*, ITMO University, Russia;
Prof. Dr. *Igor A. Tsikin*, Peter the Great St. Petersburg Polytechnic University, Russia;
Prof. Dr. *Sergey M. Ustinov*, Peter the Great St. Petersburg Polytechnic University, Russia;
Prof. Dr. *Lev V. Utikin*, Peter the Great St. Petersburg Polytechnic University, Russia.

The journal is included in the List of Leading PeerReviewed Scientific Journals and other editions to publish major findings of PhD theses for the research degrees of Doctor of Sciences and Candidate of Sciences.

Open access journal is to publish articles of a high scientific level covering advanced experience, research results, theoretical and practical problems of informatics, electronics, telecommunications, and control.

The journal is indexed by Ulrich's Periodicals Directory, Google Scholar, EBSCO, ProQuest, Index Copernicus, VINITI RAS Abstract Journal (Referativnyi Zhurnal), VINITI RAS Scientific and Technical Literature Collection, Russian Science Citation Index (RSCI) database Scientific Electronic Library and Math-Net.ru databases.

The journal is registered with the Federal Service for Supervision in the Sphere of Telecom, Information Technologies and Mass Communications (ROSKOMNADZOR). Certificate ЭЛ No. ФС77-77378 issued 25.12.2019.

Editorial office

Dr. Sc., Professor A.S. Korotkov – Editor-in-Chief;

Ph.Ch.S. Bastian – literary editor, proofreader; G.A. Pyshkina – editorial manager; A.A. Kononova – computer layout; I.E. Lebedeva – English translation.

Address: 195251 Polytekhnikeskaya Str. 29, St. Petersburg, Russia.

+7 (812) 552-6216, e-mail: infocom@spbstu.ru

Release date: 31.07.2024

© Peter the Great St. Petersburg Polytechnic University, 2024

МИНИСТЕРСТВО НАУКИ И ВЫСШЕГО ОБРАЗОВАНИЯ РОССИЙСКОЙ ФЕДЕРАЦИИ



ISSN 2687-0517

Информатика, телекоммуникации и управление

**Том 17, № 2
2024**

Санкт-Петербургский политехнический
университет Петра Великого
2024

ИНФОРМАТИКА, ТЕЛЕКОММУНИКАЦИИ И УПРАВЛЕНИЕ

РЕДАКЦИОННЫЙ СОВЕТ ЖУРНАЛА

Юсунов Р.М., чл.-кор. РАН, Санкт-Петербургский институт информатики и автоматизации РАН, Санкт-Петербург, Россия; *Арсеньев Д.Г.*, чл.-кор. РАН, д-р техн. наук, профессор, Санкт-Петербургский политехнический университет Петра Великого, Санкт-Петербург, Россия; *Воеводин В.В.*, чл.-кор. РАН, Московский государственный университет им. М.В. Ломоносова, Москва, Россия; *Заборовский В.С.*, д-р техн. наук, профессор, Санкт-Петербургский политехнический университет Петра Великого, Санкт-Петербург, Россия; *Козлов В.Н.*, д-р техн. наук, профессор, Санкт-Петербургский политехнический университет Петра Великого, Санкт-Петербург, Россия; *Фотиади А.Э.*, д-р физ.-мат. наук, профессор, Санкт-Петербургский политехнический университет Петра Великого, Санкт-Петербург, Россия; *Черноруцкий И.Г.*, д-р техн. наук, профессор, Санкт-Петербургский политехнический университет Петра Великого, Санкт-Петербург, Россия.

РЕДАКЦИОННАЯ КОЛЛЕГИЯ ЖУРНАЛА

Главный редактор

Коротков А.С., д-р техн. наук, профессор, Санкт-Петербургский политехнический университет Петра Великого, Санкт-Петербург, Россия;

Редакционная коллегия:

Дробинцев П.Д., канд. техн. наук, доцент, Санкт-Петербургский политехнический университет Петра Великого, Санкт-Петербург, Россия;

Ицыксон В.М., канд. техн. наук, доцент, Санкт-Петербургский политехнический университет Петра Великого, Санкт-Петербург, Россия;

Феррари Ф., профессор, Университет Гренобль-Альпы, Гренобль, Франция;

Краутишайдер В., профессор, Гамбургский технический университет, Гамбург, Германия;

Кучерявый Е.А., канд. техн. наук, профессор, Университет Тампере, Финляндия.

Люо Ф.-Л., University of Washington, Washington, USA;

Макаров С.Б., д-р техн. наук, профессор, Санкт-Петербургский политехнический университет Петра Великого, Санкт-Петербург, Россия;

Новаков Э., профессор, Университет Гренобль-Альпы, Гренобль, Франция;

Прокопенко Н.Н., д-р техн. наук, профессор, Донской государственный технический университет, г. Ростов-на-Дону, Россия;

Путря М.Г., д-р техн. наук, профессор, Национальный исследовательский университет «Московский институт электронной техники», Москва, Россия;

Пышкин Е.В., профессор, Университет Айзу, Айзу-Вакаматсу, Япония;

Сороцкий В.А., д-р техн. наук, профессор, Санкт-Петербургский политехнический университет Петра Великого, Санкт-Петербург, Россия;

Трифонов П.В., д-р техн. наук, доцент, Национальный исследовательский университет ИТМО, Санкт-Петербург, Россия;

Устинов С.М., д-р техн. наук, профессор, Санкт-Петербургский политехнический университет Петра Великого, Санкт-Петербург, Россия;

Уткин Л.В., д-р техн. наук, профессор, Санкт-Петербургский политехнический университет Петра Великого, Санкт-Петербург, Россия;

Цикин И.А., д-р техн. наук, профессор, Санкт-Петербургский политехнический университет Петра Великого, Санкт-Петербург, Россия;

Шкодьерев В.П., д-р техн. наук, профессор, Санкт-Петербургский политехнический университет Петра Великого, Санкт-Петербург, Россия.

Журнал с 2002 года входит в Перечень ведущих рецензируемых научных журналов и изданий, в которых должны быть опубликованы основные результаты диссертаций на соискание ученой степени доктора и кандидата наук.

Сетевое издание открытого доступа публикует статьи высокого научного уровня, освещающие передовой опыт, результаты НИР, теоретические и практические проблемы информатики, электроники, телекоммуникаций, управления.

Сведения о публикациях представлены в Реферативном журнале ВИНТИ РАН, в международной справочной системе «Ulrich`s Periodical Directory», в Российской государственной библиотеке. В базах данных: Российский индекс научного цитирования (РИНЦ), Google Scholar, EBSCO, Math-Net.Ru, ProQuest, Index Copernicus.

Журнал зарегистрирован Федеральной службой по надзору в сфере информационных технологий и массовых коммуникаций (Роскомнадзор). Свидетельство о регистрации Эл № ФС77-77378 от 25.12.2019.

Учредитель и издатель: Санкт-Петербургский политехнический университет Петра Великого, Санкт-Петербург, Российская Федерация.

Редакция журнала

д-р техн. наук, профессор А.С. Коротков – главный редактор;

Ф.К.С. Бастиан – литературный редактор, корректор; Г.А. Пышкина – ответственный секретарь, выпускающий редактор;

А.А. Кононова – компьютерная вёрстка; И.Е. Лебедева – перевод на английский язык.

Адрес редакции: Россия, 195251, Санкт-Петербург, ул. Политехническая, д. 29.

Тел. редакции +7(812) 552-62-16, e-mail редакции: infocom@spbstu.ru

Дата выхода: 31.07.2024

© Санкт-Петербургский политехнический университет Петра Великого, 2024

Contents

Information Technology

Yanchus V.E., Kukulian V.Y. The influence of highlighted text on its perception when performing interpreting from a computer screen 7

Circuits and Systems for Receiving, Transmitting, and Signal Processing

Leontiev E.V. Class G power amplifier synthesis based on the probability density function dependence of the transmitted signal 17

Computer Software, Telecommunications, and Control Systems

Varlamov D.A., Nikiforov I.V., Ustinov S.M. Algorithm for monitoring and improving the stability of the IT infrastructure based on availability and reliability metrics 24

Computer Simulations of Telecommunication, Control, and Social Systems

Timofeev S.V., Baenkhaeva A.V. A mathematical model of information confrontation: discrete adaptive control of the system 38

Gebel E.S. Approaches and principles for advanced control of multi-flow tube furnace 52

Intelligent Systems and Technologies

Shariaty F., Pavlov V.A., Surakov M.U. Comparison and selection of radiomic and deep convolutional features for improving the accuracy of CT-image texture classification 62



Содержание

Информационные технологии

Янчус В.Э., Кукульян В.Ю. Исследование влияния выделения текста цветом на эффективность его восприятия при переводе с экрана 7

Устройства и системы передачи, приема и обработки сигналов

Леонтьев Е.В. Синтез усилителя мощности класса G на основе PDF-зависимости излучаемого сигнала 17

Программное обеспечение вычислительных, телекоммуникационных и управляющих систем

Варламов Д.А., Никифоров И.В., Устинов С.М. Алгоритм мониторинга и повышения стабильности информационно-технологической инфраструктуры на основе метрик доступности и надежности 24

Моделирование вычислительных, телекоммуникационных, управляющих и социально-экономических систем

Тимофеев С.В., Баенхаева А.В. Математическая модель информационного противоборства: дискретное адаптивное управление системой 38

Гебель Е.С. Подходы и принципы усовершенствованного управления многопоточной трубчатой печью 52

Интеллектуальные системы и технологии

Шариати Ф., Павлов В.А., Сураков М.У. Сравнение и выбор радиомических и глубоких сверточных признаков для повышения точности классификации текстур КТ-изображений 62

Information Technology

Информационные технологии

Research article

DOI: <https://doi.org/10.18721/JCSTCS.17201>

UDC 004.5



THE INFLUENCE OF HIGHLIGHTED TEXT ON ITS PERCEPTION WHEN PERFORMING INTERPRETING FROM A COMPUTER SCREEN

V.E. Yanchus ✉ , *V.Y. Kukulian* 

Peter the Great St. Petersburg Polytechnic University,
St. Petersburg, Russian Federation

✉ victorimop@mail.ru

Abstract. This paper examines an experimental study of the effect of highlighted text with color underlays on the efficiency of its perception when translating from a screen. The study was conducted using eye-tracking technology and oculography methods, to analyze the perception of stimulus material by interpreters when translating from a screen. Methods of mathematical statistics were used to process the experimental data obtained. During the experiment, participants were asked to interpret from the screen sentences presented in stimuli with different options for highlighting the text with color. Factor analysis of the experimental data obtained from the eye tracker revealed statistically significant differences in text perception effectiveness depending on the combination of the investigated factors. The analysis demonstrated that the use of a serif font, a contrasting black background, and white underlay for highlighting the semantic centers of sentences can significantly improve the quality of an interpreter's work with on-screen text. The results of this study can be applied in the development and optimization of the interface design for specialized simulators and training systems for professional training of interpreters.

Keywords: eye tracking, experiment, highlighted text, text perception, translation, education, training simulator

Citation: Yanchus V.E., Kukulian V.Y. The influence of highlighted text on its perception when performing interpreting from a computer screen. *Computing, Telecommunications and Control*, 2024, Vol. 17, No. 2, Pp. 7–16. DOI: [10.18721/JCSTCS.17201](https://doi.org/10.18721/JCSTCS.17201)


Научная статья

DOI: <https://doi.org/10.18721/JCSTCS.17201>

УДК 004.5



ИССЛЕДОВАНИЕ ВЛИЯНИЯ ВЫДЕЛЕНИЯ ТЕКСТА ЦВЕТОМ НА ЭФФЕКТИВНОСТЬ ЕГО ВОСПРИЯТИЯ ПРИ ПЕРЕВОДЕ С ЭКРАНА

В.Э. Янчус  , *В.Ю. Кукульян* Санкт-Петербургский политехнический университет Петра Великого,
Санкт-Петербург, Российская Федерация victorimop@mail.ru

Аннотация. В работе рассматривается экспериментальное исследование влияния выделения текста цветом на эффективность его восприятия при переводе с экрана. Исследование проводилось с использованием методов окулографии, технологии айтрекинга для анализа восприятия стимульного материала переводчиками при переводе с экрана. Для обработки полученных экспериментальных данных использовались методы математической статистики. В ходе эксперимента участникам предлагалось выполнить перевод с экрана предложений, представленных в стимулах с различными вариантами выделения текста цветом. Факторный анализ полученных с айтрекера экспериментальных данных позволил выявить статистически значимые различия в эффективности восприятия текста в зависимости от сочетания исследуемых факторов. Анализ показал, что использование шрифта с засечками, контрастного черного фона и белого цветового выделения смысловых центров предложений может значительно улучшить качество работы переводчика при работе с экранном изображением. Результаты данного исследования могут быть применены при разработке и оптимизации дизайна интерфейса специализированных тренажеров и обучающих систем для профессиональной подготовки переводчиков.

Ключевые слова: айтрекинг, эксперимент, выделение текста, восприятие текста, перевод, обучение, обучающий тренажер

Для цитирования: Yanchus V.E., Kukulian V.Y. The influence of highlighted text on its perception when performing interpreting from a computer screen // Computing, Telecommunications and Control. 2024. Т. 17, № 2. С. 7–16. DOI: 10.18721/JCSTCS.17201

Introduction

The modern world is characterized by an increase in the volume of information and a variety of forms of its presentation. In this context, the efficiency of textual information interpretation becomes a key component in intercultural exchange of knowledge and information. Modern interpreter training methods must adapt to these conditions, integrating advanced technologies and research to improve training effectiveness. One of the tools for studying the process of interpreting textual information is eye tracking, which provides an opportunity to study the process of perception of on-screen text and interpreters' attention to various aspects of textual information. The works of S. O'Brien, C. Walker, and F.M. Federici [1, 2] have significantly influenced the development of this area of research, highlighting the potential of eye tracking in the context of interpreter training and analysis of their professional activities. These studies became the starting point for further research aimed at optimizing the translation process using eye-tracking technologies.

The use of eye tracking in the context of interpreter training is of particular significance, since it provides an opportunity to identify key aspects of text perception based on reliable parametric data of the stimulus material viewing pattern. Analysis of eye movements in real time allows not only to determine

which areas of text the subject pays special attention to, but also to analyze the sequence of perception and transitions between different parts of the text.

The aim of this study is to examine the perception of color-highlighted text by interpreters using eye-tracking technology. This research will examine the relevance of color highlighting text when interpreting from a computer screen. Analysis of experimental data obtained using eye-tracking technology is aimed at identifying statistically significant features of color-highlighted text perception.

The research objectives are:

1. To determine the factors influencing the interpreter's perception of the text.
2. To develop stimulus material.
3. To determine the task for experiment participants.
4. To process the experiment results using mathematical statistics methods.

The research hypothesis is that the use of color-highlighted text can improve the quality of an interpreter's work with on-screen text. The results obtained during this study are to be used in the development of a training simulator for translators.

Previous studies

The results of studies conducted by V.A. Demareva, S. Toldova, and K. Rayner [3, 4, 5] have provided valuable data on readers' behavioral strategies during text perception. In particular, they identified the main patterns of viewing stimulus material, indicating a saw-tooth nature of sequential text scanning. This process is predominantly carried out from left to right and from top to bottom, which corresponds to the direction of writing in the subjects' native languages. However, in the case of languages with a reverse direction of writing, a similar movement is observed in the eye movement of the subjects. These results highlight the universality of certain reading behavioral strategies applicable to various writing systems and confirm the relevance of using eye tracking for analyzing text perception in different linguistic and cultural contexts.

Eye movements during text reading represent a sequential alternation of fixations and saccades, the proportions of which are influenced by several factors:

- Complexity of the text. If the text contains complex or unfamiliar terms, phrases or constructions, the interpreter may slow down, making longer fixations for a more thorough understanding of the text.
- Presence of specialized vocabulary. Knowledge of the topic, subject area, or text specifics can speed up the reading process and reduce the length of fixations, since the interpreter more easily recognizes and understands specific terms.
- Language skills. The interpreter's language skill level affects reading speed, as well as the proportions of fixations and saccades. Experienced interpreters may use more effective text scanning strategies, which contributes to faster and more accurate perception of information [6].
- Individual characteristics of the translator. Interpreters' personal characteristics regardless of text complexity can also influence information scanning strategies during reading, creating unique patterns of fixations and saccades [7].

According to studies by Rayner and C. Clifton [5, 8], the average saccade length during text reading is 8 characters. About 15% of saccades are regressive, with a significant part of them being short, consisting of several characters. This may be because readers make too long saccades, and short regressive movements are performed to clarify information. In addition, short regressive saccades within a word may be associated with difficulties in processing the current word on which the reader's attention is focused. However, regressions longer than 10 characters indicate more serious difficulties in understanding the text, highlighting the importance of studying and analyzing regressive eye movements during reading using eye tracking for a deeper understanding of text perception mechanisms and the processes of text reading by interpreter [5].

During saccades, as well as immediately before and after them, the perception of visual information is practically absent. This time is characterized by rapid and brief eye movements, during which the eyes

move from one fixation point to another. The perception of visual information occurs precisely during fixation, when deep and detailed processing takes place. During saccades, on the contrary, low-level visual processing occurs, which emphasizes the importance of analyzing fixation time for a more complete and meaningful perception of the text in the process of reading or translation [12]. This dynamics of the visual system's operation are important when considering the relations between eye movements and the effectiveness of text perception in the process of professional interpretation of text from a computer screen.

The use of eye tracking in the field of applied linguistics and translation studies makes it possible to obtain more accurate and objective data on visual information perception by interpreters when translating text from a computer screen. This, in turn, contributes to a deeper understanding and analysis of the professional translation process, as well as optimization of interpreter training methods. One of the forms of translation considered in this study is sight translation, which involves translating a written text from the source language into spoken text in the target language [6, 9]. Discussions regarding this type of interpretation emphasize the ambiguity of its status: whether it is a separate form of interpretation or a training exercise for other forms of interpreting [11]. Eye tracking allows for a deeper investigation of this issue, providing data for objective analysis, which is an important step towards determining the role and significance of sight translation in the general context of translation practice.

Current research widely supports the concept that sight translation has several key characteristics:

- Time constraints, due to limited time for text perception and translation decision-making, as well as high speech speed, are highlighted as one of the key characteristics of this type of translation [6, 9].
- Strict self-control, which is recognized as an important aspect, requires the accuracy of the original translation, and prohibits corrections [11, 12].
- Limited access to the context of the source text, which challenges the interpreter to convey accurately the nuances and meaning of the text.

From a cognitive load perspective, sight translation represents multiple interconnected operations that the interpreter performs in parallel. With this type of translation, the interpreter must simultaneously perceive and process visual information in the source language, form an oral message in the target language, and maintain strict control over the entire process. Thus, sight translation requires the interpreter not only to know two languages, but also to be able to effectively coordinate various cognitive tasks in real time.

In her research [1], O'Brien highlights the challenge of reproducing a realistic task and environment, which significantly affects the results of experiments. She emphasizes that when conducting research on translation process, it is crucial to ensure participants' natural behavior, consistent with their usual behavior during translation practices. Given that such experiments inherently have a certain degree of artificiality, creating a comfortable environment, ensuring anonymity, and providing information about the research objectives are key to ensuring the reliability of the results. These measures aim to minimize the potential influence of stress factors or unnatural conditions on study results.

Methods and materials

At the initial stage of experiment development, factors were identified that presumably influence information perception when working with on-screen text:

- Contrast. Variations in the color contrast between background and text, represented by a black background with white text and a white background with black text.
- Highlighting the semantic centers of sentences in blue, orange, black, and white underlays.
- Font. Variations in typeface design, represented by sans-serif fonts ("PT Sans") and serif fonts ("Times New Roman").

Based on the results of a previous study, it was found that abrupt changes in background caused discomfort in participants [13, 14]. Consequently, modifications were made to the stimulus material for

The past year has witnessed **new shopping malls** in downtown Damascus.

Fig. 1. Stimulus material with white background and text written in black with orange underlay

America's mining industry injured **34 coal miners** last year.

Fig. 2. Stimulus material with black background and text written in white with blue underlay

the present experiment. To smooth the transition between stimuli and reduce participants' eyestrain, the stimuli were interspersed with gray screens. The display time for these intermediate screens was 500 ms.

Additionally, changes were made to the method of highlighting the semantic centers of sentences. Instead of bold text, colored underlays were used. This choice was based on the results of researches by M.L. Gaddy, M. Gumbrecht, and M. Yeari, highlighting the effectiveness of this method for retaining text information [15, 16, 17].

In her experimental study [15] on the impact of color-highlighted text on the perception and retention of information, Gaddy identified the following key results:

- Highlighted or underlined information was remembered significantly better by the participants in the experiment compared to non-highlighted information.
- The color of the underlays did not significantly affect memorization process.

Gumbrecht's eye-tracking study confirms that highlighted text areas play a crucial role in the perception of visual information during reading. The data obtained show that users not only pay more attention to these areas, but also actively focus their gaze on them, with approximately half of their fixations occurring on highlighted areas of the text. This finding highlights the importance of considering highlighted areas when designing digital interfaces, as it can substantially affect users' ability to effectively find and process necessary information in digital textual contexts.

Yeari's eye-tracking study on the effect of text highlighting on the processing and retention of textual information also confirms that highlighting central information with color underlays in text reduces the rereading of information in the peripheral vision zone, while highlighting peripheral information increases the rereading of this information. Other studies also confirm the statistically significant influence of this method of highlighting information in the context of memorization process [18, 19, 20].

The task for experiment participants was to translate sentences displayed on a computer screen. As a part of the experiment, stimulus material consisting of 12 sentences was developed, including various combinations of the factors described earlier (Fig. 1–2). Parametric data on the pattern of viewing stimulus material, obtained from the eye-tracker were processed using statistical analysis methods.

The experiment involved 41 student from the 4th year of bachelor's and 1st year of master's programs in linguistics at Peter the Great St. Petersburg Polytechnic University. Thirteen participants underwent the experiment in the Human-Computer Interaction Laboratory at the Higher School of Design and Architecture using the SMI RED 250 eye-tracking hardware-software complex. Twenty-eight participants took part in the experiment at the Digital Linguistics Laboratory at the Higher School of Linguistics and Pedagogy using the Tobii TX 300 eye-tracking system.

Results

The analysis of experimental data was conducted using the automated software complex "Statistics". To identify statistical dependencies, multivariate analysis of variance was used. To confirm the statistical hypotheses, a standard ANOVA procedure was performed with the significance level (p-value) set at 0.05.

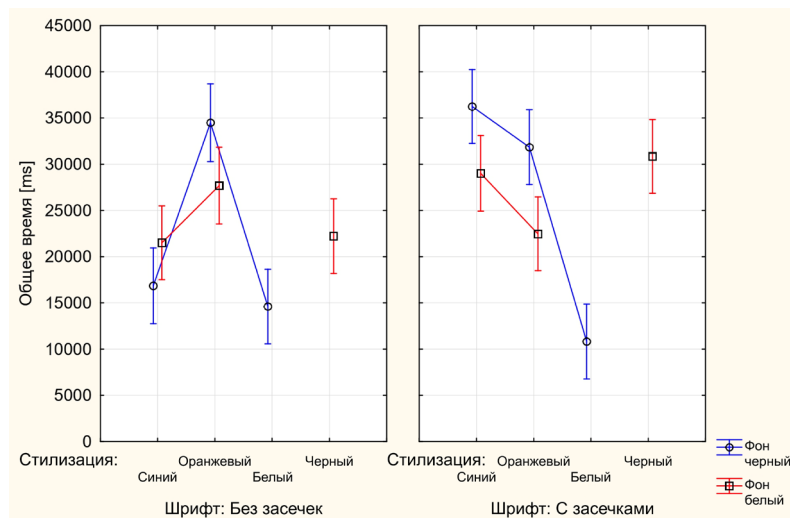


Fig. 3. Density distribution of stimulus viewing time in relation to the factors of background, highlighting, and font

Analysis of the total time spent working with the stimulus material indicates statistically significant differences in the time spent by participants on solving the experimental task when observing stimuli with various factor combinations (Fig. 3). The results show that stimuli with a black background and white underlays required the subjects the least amount of time (approximately 10000 ms) to solve the problem. This aligns with expectations based on previous research and confirms that certain combinations of factors can significantly influence text perception time [14].

The p-value obtained through statistical analysis confirms the statistical significance of differences in total working time when using various combinations of style and font factors (Table 1).

Table 1
p-value obtained as a result of ANOVA program procedure for the parameter “Total amount of time”

	p-value
Contrast	
Highlight	0,028
Font	
Contrast * Highlight	0,02
Contrast * Font	
Highlight * Font	< 0,0001
Contrast * Highlight * Font	0,113

However, an interesting result is the revealed influence of colored underlays. In particular, subjects solved the experimental problem faster when working with stimuli featuring a black background with white underlays compared to stimuli with a black background and orange underlays. The latter required significantly more time from participants (about 30000–35000 ms). Stimuli with blue underlays were second in terms of task solution speed, but only in the case of stimuli with sans-serif fonts, similarly on a black background (Table 1).

When working with stimuli on a white background, participants required an average time of 20000–30000 ms. However, despite the increase in working time with stimuli, the general trend remains. Working

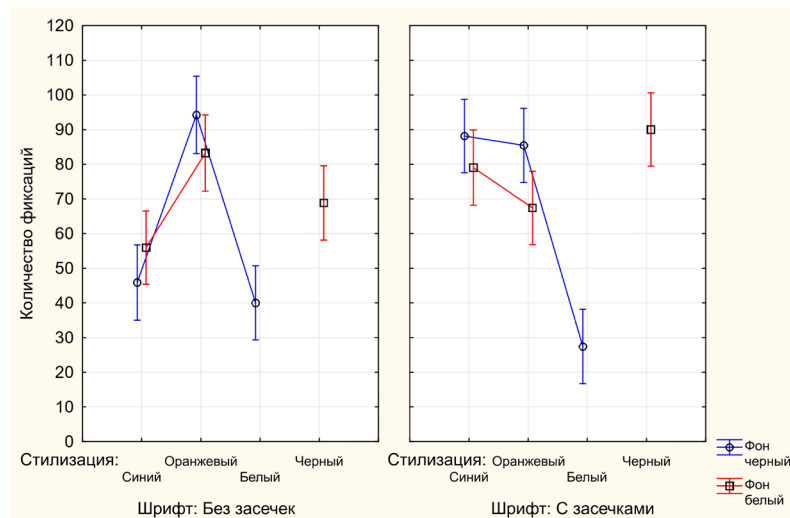


Fig. 4. Density distribution of the number of fixations during stimulus viewing in relation to the factors of background, highlighting, and font

time with stimuli reduces when using serif fonts and orange underlays, and when using sans-serif fonts and blue underlays. At the same time, the most contrasting black underlay on a white background did not result in a significant increase in the speed of solving problems, as was the case with the reverse contrast (black background and white underlays).

Analysis of the number of fixations when working with the stimulus material indicates the smallest number of fixations when using a black background, serif font, and white underlays (Fig. 4). This may indicate an increase in the speed of perception and rapid text scanning of text in this stimulus configuration. The black background and contrasting white underlays in the stimuli likely contribute to the ease of distinguishing text elements.

The results of the statistical analysis, based on p-values, indicate the statistical significance of differences in the number of fixations depending on the use of various combinations of highlighting and font factors (Table 2).

Table 2

p-value obtained as a result of ANOVA program procedure for the parameter “Quantity of fixations”

	p-value
Contrast	
Highlight	< 0,0001
Font	
Contrast * Highlight	0,053
Contrast * Font	
Highlight * Font	< 0,0001
Contrast * Highlight * Font	0,435

Conversely, the maximum number of fixations was observed when using stimuli with a black background, sans-serif font, and orange underlays. This may indicate a more complex perception of the text in this configuration, possibly due to the absence of serifs in the font and a more intense color contrast between the text and the underlays.

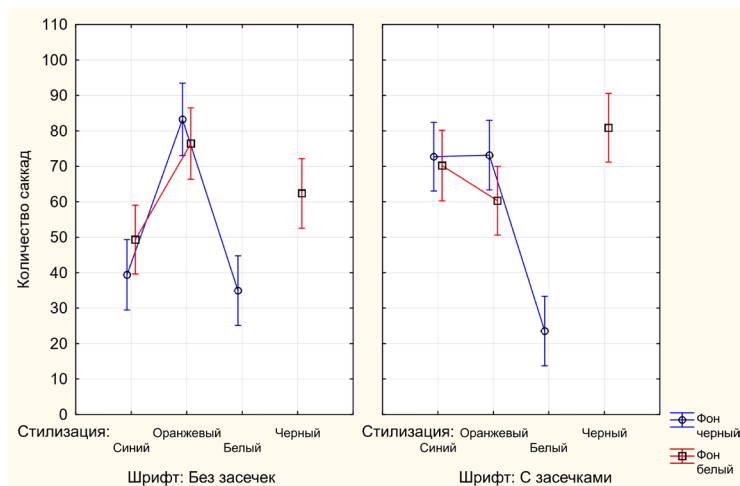


Fig. 5. Density distribution of the number of saccades during stimulus viewing in relation to the factors of background, highlighting, and font

Any combination of factors with a white background results in average fixation values. This may indicate that while a white background provides some contrast, it still reduces the level of visual impact compared to a black background.

Analysis of the number of saccades when working with stimulus material shows trends similar to the analysis of fixations shown in Fig. 5. In the case of a black background, serif font, and white underlays, the number of saccades corresponds to the minimum number of fixations. This indicates efficient text scanning and a minimum number of necessary eye movements.

Statistical analysis of the number of saccades when working with the stimulus material also confirms that the chosen method of text highlighting and font type influence the process of text perception (Table 3).

Table 3

p-value obtained as a result of ANOVA program procedure for the parameter “Quantity of saccades”

	p-value
Contrast	
Highlight	< 0,0001
Font	
Contrast * Highlight	0,057
Contrast * Font	
Highlight * Font	< 0,0001
Contrast * Highlight * Font	0,057

In a situation with a black background, sans-serif font, and orange underlays, the number of saccades increases rapidly. This aligns with the large number of fixations in this configuration and may indicate more complex text perception, requiring a more corrections and transitions between fixation points. The white background factor, in combinations with various text highlighting techniques and fonts, confirms the conclusions drawn from the analysis of fixations.

Conclusion

Based on the conducted research, a statistical dependence of text perception on background color was revealed. It was established that under certain conditions, the speed of information perception increases

on a black background. It was determined that the highest speed of information perception is achieved when text is highlighted with a white underlay on a black background, which is confirmed by statistically significant differences in the total amount of time for solving the experimental problem, the number of fixations and saccades. The statistical significance of the influence of font type on the process of text perception was also revealed. The results of this study can be used to optimize training materials in the interfaces of translator simulators, ensuring the effectiveness of their work.

REFERENCES

1. **O'Brien S.** Eye tracking in translation process research: methodological challenges and solutions. *Copenhagen studies in language*, 2009, pp. 251–266.
2. **Walker C., Federici F.M.** Eye tracking and multidisciplinary studies on translation. Amsterdam: John Benjamins Publishing Company, 2018. 301 p.
3. **Demareva V.A., Golubinskaya A.V., Mayasova T.V., Vyakhireva V.V., Zhukova M.V., Golubin R.V.** Psychophysiological Markers of Epistemic Evaluation: Evidence from Eye Tracking in Reading Familiar and Unfamiliar Words. *Opera Medica et Physiologica*, 2021, Vol. 8, no. 4, pp. 41–48. DOI: 10.24412/2500-2295-2021-4-41-48
4. **Toldova S., Slioussar N., Bonch-Osmolovskaya A.** Discourse complexity in the light of eye-tracking: a pilot Russian language study. *Russian Journal of Linguistics*, 2022, Vol. 26, no. 2, pp. 449–470. DOI: 10.22363/2687-0088-30140
5. **Rayner K.** Eye movements in reading and information processing: 20 years of research. *Psychological Bulletin*, 1998, Vol. 124, no. 3, pp. 372–422. DOI: 10.1037/0033-2909.124.3.372
6. **Kokanova E., Lyutyanskaya M., Cherkasova A.** Eye tracking study of reading for translation and English-Russian sight translation. *Translation, interpreting, cognition: The way out of the box*. Berlin: Language Science Press, 2021, pp. 163–171. DOI: 10.5281/zenodo.4545045
7. **Bausela M.B., De Wille T.** An Eye-Tracking Study of Cognitive Effort in Processing of Lexical Features in Students and Experts. *Hikma*, 2023, Vol. 22, no. 1, pp. 219–248. DOI: 10.21071/hikma.v22i1.15063
8. **Clifton C., Ferreira F., Henderson J.M., Inhoff A.W., Liversedge S.P., Reichle E.D., Schotter E.R.** Eye movements in reading and information processing: Keith Rayner's 40year legacy. *Journal of Memory and Language*, 2016, Vol. 86, pp. 1–19. DOI: 10.1016/j.jml.2015.07.004
9. **Kokanova E.S., Lyutyanskaya M.M., Cherkasova A.A.** Eye Tracking Study of Reading and Sight Translation. *SHS Web of Conferences*, 2018, Vol. 50, Article no. 01080. DOI: 10.1051/shsconf/20185001080
10. **Frash S.S., Maksyutina O.V.** Sight translation as an independent branch of translation. *Tomsk State Pedagogical University Bulletin*, 2010, Vol. 4, pp. 76–81
11. **Chmiel A., Mazur I.** Eye tracking sight translation performed by trainee interpreters. *Tracks and treks in translation studies*, 2013, pp. 189–205. DOI: 10.1075/btl.108.10chm
12. **Thawabteh M.A.** Difficulties of sight translation: Training translators to sight translate. *Current Trends in Translation Teaching and Learning*, 2015, Vol. 2, pp. 171–195.
13. **Kukulian V., Yanchus V.** Development of a methodology for investigating the perception of stylized text in the process of professional translation using eye-tracking technology. *Computing for Physics and Technology (CPT2024)*, 2023, pp. 103–111. DOI: 10.54837/9785604289174_CPT2023-p103
14. **Kukulian V.Y., Yanchus V.E.** Investigating the Perception of Stylized Text in the Process of Professional Translation Using Eye-tracking. *Graphic Information Systems and Immersive Technologies in the Product Life Cycle Stages (GraphiCon 2023)*, 2023, Vol. 33, pp. 938–947. DOI: 10.20948/graphicon-2023-938-947
15. **Gaddy M.L.** Studying from highlighted material: the role of color in memory for text. *Master's Theses*, 1996. Article no. 1226. DOI: 10.31979/etd.qp9n-n73d

16. **Chi E.H., Gumbrecht M., Hong L.** Visual Foraging of Highlighted Text: An Eye-Tracking Study. Human-Computer Interaction. HCI Intelligent Multimodal Interaction Environments. Lecture Notes in Computer Science, 2007, Vol. 4552, pp. 589–598. DOI: 10.1007/978-3-540-73110-8_64

17. **Yeari M., Oudega M., van den Broek P.** The effect of highlighting on processing and memory of central and peripheral text information: evidence from eye movements. Journal of Research in Reading, 2017, Vol. 40, no. 4, pp. 365–383. DOI: 10.1111/1467-9817.12072

18. **Ponce H.R., Mayer R.E.** An eye movement analysis of highlighting and graphic organizer study aids for learning from expository text. Computers in human behavior, 2014, Vol. 41, pp. 21–32. DOI: 10.1016/j.chb.2014.09.010

19. **Ben-Yehudah G., Eshet-Alkalai Y.** The contribution of text-highlighting to comprehension: A comparison of print and digital reading. Journal of Educational Multimedia and Hypermedia, 2018, Vol. 27, no. 2, pp. 153–178.

20. **Mason L., Ronconi A., Carretti B., Nardin S., Tarchi C.** Highlighting and highlighted information in text comprehension and learning from digital reading. Journal of Computer Assisted Learning, 2024, Vol. 40, no. 2, pp. 637–653. DOI: 10.1111/jcal.12903

INFORMATION ABOUT AUTHORS / СВЕДЕНИЯ ОБ АВТОРАХ

Yanchus Victor E.

Янчус Виктор Эдмундасович

E-mail: victorimop@mail.ru

Kukulian Victoria Y.

Кукутьян Виктория Юрьевна

E-mail: kukulyan.vyu@edu.spbstu.ru

ORCID: <https://orcid.org/0009-0001-0503-3261>

Submitted: 13.04.2024; Approved: 20.06.2024; Accepted: 15.07.2024.

Поступила: 13.04.2024; Одобрена: 20.06.2024; Принята: 15.07.2024.

Circuits and Systems for Receiving, Transmitting and Signal Processing

Устройства и системы передачи, приема и обработки сигналов

Research article

DOI: <https://doi.org/10.18721/JCSTCS.17202>

UDC 621.375.026



CLASS G POWER AMPLIFIER SYNTHESIS BASED ON THE PROBABILITY DENSITY FUNCTION DEPENDENCE OF THE TRANSMITTED SIGNAL

E.V. Leontiev  

Peter the Great St. Petersburg Polytechnic University,
St. Petersburg, Russian Federation

 evgeniyleo888@mail.ru

Abstract. The article describes the technique of parametric synthesis of a class G power amplifier with maximum drain efficiency at the average output power with high PAPR (peak to average power ratio). The proposed technique was applied to an advanced OFDM signal of LTE standard. The optimal parameters of the envelope amplifier for LTE signal were received on the basis of proposed theoretical calculation. Proposed technique validity was confirmed experimentally by measuring the 3-level class G power amplifier prototype. The prototype operates in the frequency range of 700–1000 MHz and has a maximum power 44.3 dBm. It also has a drain efficiency of 30% at power output back-off equal to the peak to average power ratio of LTE signal. From the consistency of the computational and experimental results, it is possible to predict increasing a drain efficiency from 30% to 39.5% by using the digital pre-distortion system and the 5-level envelope amplifier.

Keywords: class G power amplifier, PDF, drain efficiency, OFDM, LTE

Citation: Leontiev E.V. Class G power amplifier synthesis based on the probability density function dependence of the transmitted signal. *Computing, Telecommunications and Control*, 2024, Vol. 17, No. 2, Pp. 17–23. DOI: 10.18721/JCSTCS.17202

Научная статья

DOI: <https://doi.org/10.18721/JCSTCS.17202>

УДК 621.375.026



СИНТЕЗ УСИЛИТЕЛЯ МОЩНОСТИ КЛАССА G НА ОСНОВЕ PDF-ЗАВИСИМОСТИ ИЗЛУЧАЕМОГО СИГНАЛА

Е.В. Леонтьев 

Санкт-Петербургский политехнический университет Петра Великого,
Санкт-Петербург, Российская Федерация

✉ evgeniyleo888@mail.ru

Аннотация. Статья посвящена методике параметрического синтеза усилителя мощности класса G с максимальным КПД при средней мощности излучаемого сигнала с высоким пик-фактором. В работе показано применение предложенной методики к передовому OFDM-сигналу стандарта LTE. Получены оптимальные параметры усилителя огибающей в схеме усилителя мощности класса G для LTE-сигнала на основании теоретического расчета. Обоснованность изложенной методики подтверждена экспериментально путем измерения разработанного прототипа усилителя мощности класса G с тремя уровнями коммутации напряжения питания. Прототип работает в частотном диапазоне 700–1000 МГц, имеет максимальную мощность 44,3 дБм и КПД 30% при отстройке от максимальной мощности на величину пик-фактора LTE-сигнала. Из согласованности результатов расчет и эксперимента возможно предсказать, что при использовании системы предсказаний и усилителя огибающей с пятью уровнями коммутации напряжения питания КПД возможно увеличить с 30% до значения 39,5%.

Ключевые слова: усилитель мощности класса G, PDF, КПД, OFDM, LTE

Для цитирования: Leontiev E.V. Class G power amplifier synthesis based on the probability density function dependence of the transmitted signal // Computing, Telecommunications and Control. 2024. Т. 17, № 2. С. 17–23. DOI: 10.18721/JCSTCS.17202

Introduction

The problem of designing power amplifier (PA) with high efficiency for signals with high peak to average power ratio (PAPR) exists for a long time. Linearity and efficiency are trade-off parameters in PA design. The rapid digital electronics development has enabled implementation of the digital pre-distortion (DPD) system, which in turn has changed the trade-off between linearity and efficiency towards high efficiency. With the advent of DPD systems it becomes possible to use such PAs as the Doherty amplifier.

Doherty amplifier or other PAs with load modulation technique [1, 2] can be realized in a narrow frequency rang. PA with a supply modulation technique such as envelope tracking power amplifier (ET-PA) [3, 4] is the most interesting solution for high bandwidth task. A special case of ET-PA is a class G PA [5, 6] that has a supply modulation between discreet levels. The class G PA has high efficiency of the envelope amplifier, because it works in a pulse mode.

Now, there are some scientific articles describing class G PAs with 2, 3 or 8 supply levels [5, 6]. However, the task of determining the optimal parameters for maximum efficiency at average signal power is steel open. This work is a continuation of work [7] proposing the class G power amplifier synthesis based on a transmitted signal complementary cumulative distribution function (CCDF). Further development of this synthesis technique described in this work has determined the final theoretical basis used a probability density function (PDF) for the parametric synthesis of a class G PA, confirmed by experiment.

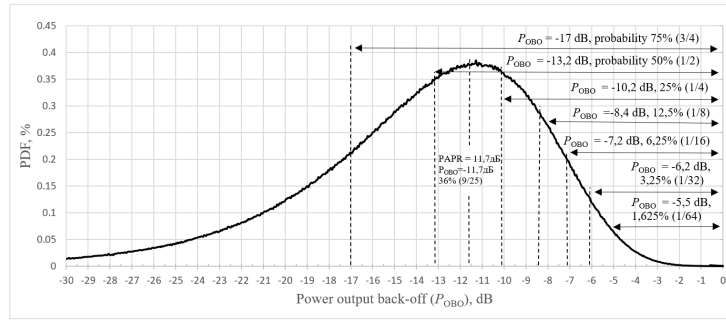


Fig. 1. PDF for LTE signal

PDF analyses

Work [7] shows that class G PA efficiency must be calculated using PDF and measurements of the main PA at discrete supply voltages. PDF determines the detecting probability of particular supply voltage level. For probability analysis, two functions are most often used: PDF and CCDF. CCDF doesn't have information about the detecting probability for signal with power less than average level. The proposed CCDF-based efficiency analysis technique [7] isn't able to determine the maximum efficiency at PA parameters that depends on the integral probability.

Fig. 1 shows probability function for the OFDM signal of LTE standard E-TM3.1 test configuration.

In order for the efficiency synthesis technique to be independent of parameters of the main PA, it is advisable to normalize the output power by maximum PA power. This normalized value is called "the power output back-off" (P_{OBO}). Integrating the PDF in specified intervals gives the opportunity to determine the probability density of signal power occurring in the selected interval.

Let us suppose that the class G PA has two switching supply voltage levels U_1 and U_2 . The supply voltage will be able to change by using a comparator. The comparator will change the supply voltage when power exceed some reference value (P_{REF}). Let P_{REF} correspond to $P_{OBO} = -11.7$ dB then, according to Fig. 1, the main amplifier will be at U_1 74% of time, and at U_2 – 36% of time. It is better to select U_1 and U_2 values at which the main PA will provide the required maximum powers for the given P_{OBO} intervals. Measuring the efficiency of the main PA for the found supply voltages allows to determine the drain efficiency (DE) of the overall class G PA using the following formula:

$$DE(\%) = 100\% \left(p(U_1) DE(P_{avg1}(W), U_1) + p(U_2) DE(P_{avg2}(W), U_2) \right), \quad (1)$$

where $p(U_N)$ is integral probability in a given interval corresponding to the supply voltage U_N ; $DE(P_{avgN}, U_N)$ is measurements of the drain efficiency of the main PA for P_{avgN} , given in Watts, and corresponding to the supply voltage U_N . In its turn, the average power for a certain interval can be calculated using the next formula:

$$P_{avgN}(W) = \frac{\sum_{i=N_k}^{N_m} 0.001W \cdot 10^{\frac{P_M(dBm) + P_{OBO_i}(dB)}{10}} PDF(P_{OBO_i})}{\sum_{i=N_k}^{N_m} PDF(P_{OBO_i})}, \quad (2)$$

where P_M is instantaneous power obtained as a result of the reverse transition from the normalized P_{OBO} value to the output signal power; $PDF(P_{OBO})$ is PDF value at P_{OBO_i} ; $[U_k, U_m]$ is interval with constant supply voltage U_N .

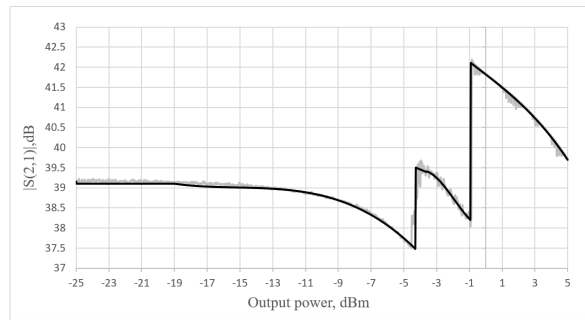


Fig. 2. Gain module

Calculating the efficiency at an average signal power allows to select such PA parameters at which the maximum efficiency value can be achieved. These parameters include: the integral probability ($p(U_N)$), which is determined by the reference voltage of the comparators; N -level supply voltage (U_N); the number of supply voltage levels (N).

Let us analyze the DE for the main PA made on LDMOS technology with a maximum power of 47 dBm at a supply voltage of 28 V. The number of supply voltage levels $N = 5$ is the optimal value for LTE signal, because the DE of class G PA is close to the maximum value 44.5% achieving in ETPA. The optimal parameters of a class G PA with five supply voltage levels are shown in Table 1.

Table 1

The optimal envelop amplifier parameters

Level number (N)	1	2	3	4	5
$U_N, \%$	6.5	7.5	10.6	13.5	28
$p(U_N), \%$	50	14	29.7	4.7	1.6
P_{avgN}, dBm	30.3	34.6	37	37.3	42
$DE(P_{avgN}, U_N), \%$	39	47	49	48	38

Note, that it is needed to use the PDF of the output signal for analysis. The PA is a nonlinear element, therefore, without a DPD system, the output signal has distortion. The PDF will be curved in this case, so this technique is applicable only with DPD system.

Class G PA distortion analyses

Fig. 2 and 3 show the measuring results of a complex transfer function for the 3-level class G PA prototype, developed in [7], and matched in 700–1000 MHz frequency range with a maximum output power of 44.3 dBm at a supply voltage 28 V.

Fig. 2 and 3 show the measurement results approximated by a piecewise polynomial sequence. When the supply voltage changes, the transfer function is discontinuing and, therefore, cannot be approximated by Taylor series. Accordingly, the transfer function of a Volterra series of DPD system is not suitable for class G PA. Today, there are some works [8, 9] describing the implementation of DPD technique for class G PA.

Based on the piecewise polynomial approximation data, a model of PA prototype was built in the VSS AWR software environment and PDF of output signal was analyzed. Fig. 4 shows the probability function for an average signal power of 33 dBm.

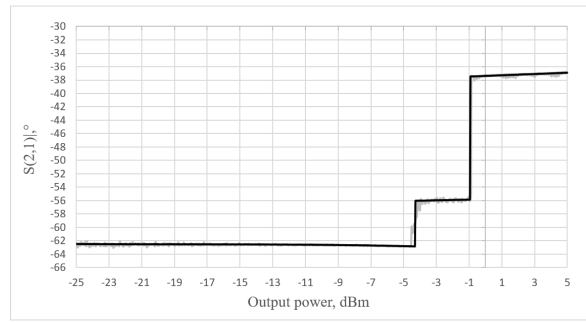


Fig. 3. Gain phase

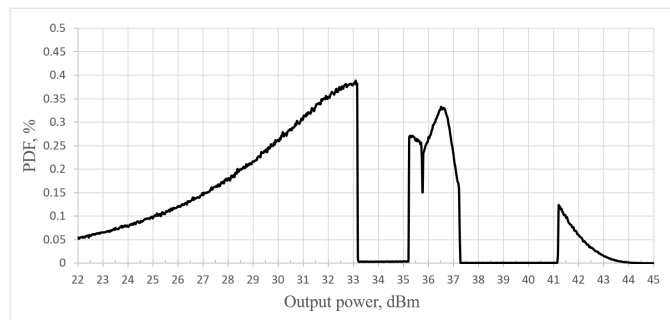


Fig. 4. PDF for $P_{avg} = 33$ dBm

The PDF has areas where the PDF is zero, because the power gain increases sharply when supply voltage changes. There is also distortion in the graph caused by gain compression at each supply voltage.

Class G PA is an element with a high level of nonlinear distortion. The ACPR of 33 dBm output signal is -22 dBc. However, all amplifier architectures solving the problem of low DE at signals with high PAPR need to correct additional DPD technique. For example, LTE standard has ACPR requirement less than -50 dBc. Table 2 provides the typical ACPR and DE for popular PA architectures.

Table 2

Parameters of different PA architectures

PA architectures	ACPR, dBc	DE, %	References
Doherty PA	$-30 \div -35$	35 – 60	[1, 2]
ETPA	$-32 \div -40$	26 – 40	[3, 4]
Class G PA	$-20 \div -25$	38 – 43	[5, 6]
Class G PA	-22	44.3	this work

Prototype measurements results

Optimal parameters for achieving maximum efficiency for $P_{avg} = 32.5$ dBm were calculated. At this moment, DPD system is not developed, therefore, we use PDF for output signal with distortion for DE analysis. A comparison of the measurement and calculation results is shown in Fig. 5.

A comparison of the calculation and experimental results shows that at an output power of 30.5 dBm and above, the measured efficiency value approaches the calculated one, which indicates the

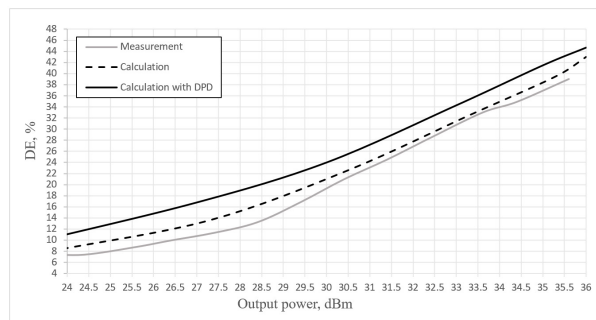


Fig. 5. Measurement results

high efficiency of the envelope amplifier in the prototype. In this output power range, the supply voltage begins to switch between three levels, while at a power below 30.5 dBm only supply voltage U_1 prevails. The current in U_1 circuit flows through the diode with the drop voltage by 0.77 V, which leads to efficiency decreasing of the envelope amplifier.

Fig. 5 also shows the dependence of the possible DE of the prototype with the DPD system. Calculations show that DPD system can increase the efficiency by 3%. It is possible to predict that the DE of the class G prototype for the number of switching levels (N) is 5. Finally, with $N = 5$ and using a DPD system, the prototype will have expected DE equal to 39.5%.

Conclusion

The class G PA is a relevant solution for the problem of PA synthesizing in a wide operating frequencies range. The technique presented in this work allows synthesize a class G PA with maximum efficiency for signals with the certain structure. This article shows that synthesis of 5-levels class G PA for advanced OFDM signals is optimal.

At the moment, a search of DPD system design technique for class G PA is still ongoing. Also, it is relevant to implement the envelope amplifier in an integrated design for improving the frequency properties and reducing the response time.

REFERENCES

1. Pelk M.J., Neo W.C.E., Gajadharsing J.R., Pengelly R.S., de Vreede L.C.N. A high-efficiency 100-W GaN three-way Doherty amplifier for base-station applications. *IEEE Transactions on Microwave Theory and Techniques*, 2008, Vol. 56, no. 7, pp. 1582–1591. DOI: 10.1109/TMTT.2008.924364
2. Serhan A. et al. A reconfigurable SOI CMOS Doherty power amplifier module for broadband LTE high-power user equipment applications. *IEEE Radio Frequency Integrated Circuits Symposium (RFIC)*, 2020, pp. 79–82. DOI: 10.1109/RFIC49505.2020.9218305
3. Balteanu F., Modi H., Khesbak S., Drogi S., DiCarlo P. Envelope tracking LTE multimode power amplifier with 44% overall efficiency. *IEEE Asia Pacific Microwave Conference (APMC)*, 2018, pp. 37–40. DOI: 10.1109/APMC.2017.8251371
4. Chen Z. et al. An open loop digitally controlled hybrid supply modulator achieving high efficiency for envelope tracking with baseband up to 200-MHz. *IEEE Transactions on Circuits and Systems I: Regular Papers*, 2020, Vol. 67, no. 11, pp. 4142–4153. DOI: 10.1109/TCSI.2020.3014087
5. Wolff N., Heinrich W., Bengtsson O. Highly efficient 1.8-GHz amplifier with 120-MHz class-G supply modulation. *IEEE Transactions on Microwave Theory and Techniques*, 2017, Vol. 65(12), pp. 5223–5230. DOI: 10.1109/TMTT.2017.2769089

6. **Florian C., Cappello T., Paganelli R.P., Niessen D., Filicori F.** Envelope tracking of an RF high power amplifier with an 8-level digitally controlled GaN-on-Si supply modulator. *IEEE Transactions on Microwave Theory and Techniques*, 2015, Vol. 63, no. 8, pp. 2589–2602. DOI: 10.1109/TMTT.2015.2447552
7. **Leontiev Ye.V., Korotkov A.S., Matveev Yu.A.** Class G power amplifier for infocommunication systems. *Nanoindustry*, 2022, Vol. 15, no. 6, pp. 368–375. DOI: 10.22184/1993-8578.2022.15.6.368.375
8. **Afsardoost S., Eriksson T., Fager C.** Digital predistortion using a vector-switched model. *IEEE Transactions on Microwave Theory and Techniques*, 2012, Vol. 60, no. 4, pp. 1166–1174. DOI: 10.1109/TMTT.2012.2184295
9. **Zhu A., Draxler P.J., Hsia C., Brazil T.J., Kimball D.F., Asbeck P.M.** Digital predistortion for envelope-tracking power amplifiers using decomposed piecewise Volterra series, *IEEE Transactions on Microwave Theory and Techniques*, 2008, Vol. 56, no. 10, pp. 2237–2247, DOI: 10.1109/TMTT.2008.2003529

INFORMATION ABOUT AUTHOR / СВЕДЕНИЯ ОБ АВТОРЕ

Leontiev Evgeniy V.

Леонтьев Евгений Владимирович

E-mail: evgeniyleo888@mail.ru

ORCID: <https://orcid.org/0000-0002-1477-3181>

Submitted: 02.06.2024; Approved: 15.07.2024; Accepted: 30.07.2024.

Поступила: 02.06.2024; Одобрена: 15.07.2024; Принята: 30.07.2024.

Software of Computer, Telecommunications and Control Systems

Программное обеспечение вычислительных, телекоммуникационных и управляющих систем

Research article

DOI: <https://doi.org/10.18721/JCSTCS.17203>

UDC 004.052.3



ALGORITHM FOR MONITORING AND IMPROVING THE STABILITY OF THE IT INFRASTRUCTURE BASED ON AVAILABILITY AND RELIABILITY METRICS

D.A. Varlamov, I.V. Nikiforov  , S.M. Ustinov 

Peter the Great St. Petersburg Polytechnic University,
St. Petersburg, Russian Federation

 igor.nikiforov@gmail.com

Abstract. Most companies have their own IT infrastructure that consists of complex systems and services. The stability of systems and services is important for companies, as problems with them can lead to loss of resources and human time. Thus, it is important to analyze previous IT service outages, which aims to identify and adjust the most critical and vulnerable elements of the infrastructure that are prone to breakage or failure. *Research objective* is to develop a new algorithm for improving the stability of IT infrastructure of a company by analyzing and taking into account the statistics of previous services outages. *As a result*, a new algorithm is proposed to identify and fix problems in IT services before they lead to serious consequences and reduce the time to find the source of problem. The algorithm is based on two new metrics: availability and reliability, which distinctive feature is the consideration of statistics of previous failures and outages in the system. The architecture of a high-performance software tool that allows real-time monitoring and evaluation of IT services stability metrics is presented. The effectiveness of the proposed algorithm is demonstrated by implementing it in a software tool and observing the growth of stability indicators – availability and reliability – after the detection and elimination of a weak link in IT services. The use of the developed algorithm allowed to reduce the time during which the material and human resources of the company were idle by 25%. The practical significance of the presented algorithm was tested in one of the large industrial information technology companies with more than 10000 employees. Based on the information obtained with created software, it was possible to obtain recommendations for improving the stability of company’s IT services.

Keywords: metrics, availability, reliability, stability, IT infrastructure, outage, monitoring

Citation: Varlamov D.A., Nikiforov I.V., Ustinov S.M. Algorithm for monitoring and improving the stability of the IT infrastructure based on availability and reliability metrics. Computing, Telecommunications and Control, 2024, Vol. 17, No. 2, Pp. 24–37. DOI: 10.18721/JCSTCS.17203

Научная статья

DOI: <https://doi.org/10.18721/JCSTCS.17203>

УДК 004.052.3



АЛГОРИТМ МОНИТОРИНГА И ПОВЫШЕНИЯ СТАБИЛЬНОСТИ ИНФОРМАЦИОННО-ТЕХНОЛОГИЧЕСКОЙ ИНФРАСТРУКТУРЫ НА ОСНОВЕ МЕТРИК ДОСТУПНОСТИ И НАДЕЖНОСТИ

Д.А. Варламов, И.В. Никифоров , С.М. Устинов 

Санкт-Петербургский политехнический университет Петра Великого,
Санкт-Петербург, Российская Федерация

 igor.nikiforov@gmail.com

Аннотация. Большинство компаний имеют собственную информационно-технологическую инфраструктуру, состоящую из сложных систем и сервисов. Стабильность работы сервисов важна для компаний, так как проблемы с ними приводят к потерям ресурсов и человеческого времени. Поэтому важным является анализ предыдущих отключений сервисов, который направлен на выявление и налаживание уязвимых элементов инфраструктуры, подверженных поломке или отказу. *Цель исследования:* разработать алгоритм для повышения стабильности информационно-технологической инфраструктуры предприятия за счет анализа и учета статистики предыдущих отключений. *Результаты:* предложен новый алгоритм, позволяющий выявлять и устранять проблемы в информационно-технологических сервисах предприятия до того, как они приведут к серьезным последствиям, и сокращать время на поиск источника проблемы. Алгоритм основан на двух новых метриках: доступность и надежность, — отличительной особенностью которых является учет статистики предыдущих отключений. Представлена архитектура высокопроизводительного программного средства, позволяющего в режиме реального времени осуществлять мониторинг и оценку показателей стабильности сервисов. Демонстрируется эффективность предложенного алгоритма путем его реализации в программном средстве и наблюдения роста показателей стабильности — доступности и надежности — после обнаружения и устранения слабого звена в информационно-технологических сервисах. Использование разработанного алгоритма позволило на 25% сократить время, в течение которого материальные и человеческие ресурсы компании простаивали. *Практическая значимость:* представленный алгоритм применен на практике в одной из крупных промышленных информационно-технологических компаний с более чем 10000 сотрудников. На основе информации, полученной при помощи созданного программного средства, удалось получить рекомендации по повышению стабильности информационных сервисов компании.

Ключевые слова: метрики, доступность, надежность, стабильность, информационно-технологическая инфраструктура, отключение, мониторинг

Для цитирования: Varlamov D.A., Nikiforov I.V., Ustinov S.M. Algorithm for monitoring and improving the stability of the IT infrastructure based on availability and reliability metrics // Computing, Telecommunications and Control. 2024. Т. 17, № 2. С. 24–37. DOI: 10.18721/JCSTCS.17203

Introduction

Stability of internal services is important for all companies using information technology infrastructure. The stability of IT services affects the speed and quality of work of all employees of the company [1]. Any downtime of services entails costs and losses for the company. Analysis of previous IT service outages is designed to find the most critical and vulnerable infrastructure elements that are prone to breakage or failure to predict in advance which of the elements have a greater probability of failure [2]. This process allows you to solve problems in the infrastructure before they lead to huge resource and human time losses as it reduces the time to find the source of the problem. That is why it is urgent to create, improve and

automate algorithms to increase the stability of the IT infrastructure [3, 4]. The main components of the IT infrastructure that stand out in our work are software, hardware, and computer networks.

The article [5] proposes to assess the stability of the IT infrastructure based on user perception. The authors suggest using one metric to assess stability: availability. Various options for calculating this metric are offered, including those that take into account the severity of failures. In our work, we propose to use not one, but two metrics to assess the stability of the IT infrastructure: availability and reliability. We distinguish two classes of problems with the IT infrastructure: outage and degradation. Outage refers to a condition in which the service cannot perform its basic functionality. Degradation refers to a condition in which the service is able to perform its basic functions, but some of the additional functions cease to work correctly. We cannot use a single metric to evaluate a system that can be in one of three states: healthy, degrading or failing, because it is unclear to what extent degradation and to what extent outages will affect it. We need to have two metrics: one will only be affected by outages, and the second one will be affected by degradations and outages. Considering both classes of problems, the combination of the two metrics will give us a more informative assessment of IT infrastructure stability.

The goal of the work is to develop and implement in the software a new algorithm for improving the stability of IT infrastructure, a distinctive feature of which is the accounting of statistics of previous outages. To achieve this goal in the work, it is required to perform the tasks listed below.

1. To study existing solutions to improve IT infrastructure stability.
2. To study existing algorithms to calculating key indicators of IT infrastructure stability.
3. To propose a new algorithm for calculating key indicators of IT infrastructure stability, taking into account the state of degradation.
4. To propose the algorithm for improving stability of IT infrastructure. A distinctive feature of the algorithm is the accounting of statistics of previous outages.
5. Implement the proposed algorithm in a software tool.
6. Evaluate the effectiveness of the developed algorithm and the software that implements it.

Overview of solutions to improve stability

There are various algorithms for improving stability. For example, in the article [6] authors consider an algorithm to increase the stability of IT services in large companies with overlapping IT frameworks. To improve the quality of IT services, they propose to use a combination of reliability, assurance, responsiveness, empathy and tangibles to improve the quality of services. However, they focus on providing IT services as a service, and in our article, we focus specifically on IT infrastructure within the company.

The article [7] describes an algorithm for monitoring and measuring the quality for the Internet of Services (IoS) – an ecosystem in which online and offline services provided by many different service providers are intertwined. The authors developed and implemented an algorithm based on establishing a hierarchy of indices divided into three types: value, quality and capability (VQC). After dividing indices, service providers establish a dynamic hierarchy that defines the calculation relationship between indices, which helps to monitor the stability of the system in real time. This algorithm is effective when it comes to integrating services from different service providers. However, the company's IT infrastructure often has one or very few service providers, and in this case, the advantages of the VQC algorithm, tailored for IoS, are not fully used.

The article [8] contains various approaches to using machine learning to improve the security and stability of power systems. Machine learning allows you to quickly identify and detect problems related to cyberattacks, voltage instability, power quality disturbance, etc. The article discusses various algorithms to the implementation of machine learning: artificial neural networks (ANN), decision tree (DT), support vector machines (SVM). The same algorithms can be used not only to improve the stability of power systems, but also to apply them to IT systems. However, machine learning methods have a number of disadvantages: firstly, a large amount of data is needed for training the model. It may take

years to collect enough data for datasets from monitoring systems. Secondly, they have low estimation accuracy and often make mistakes, and therefore are poorly applicable in big IT systems where the price of mistake is very high.

In the article [9], the authors proposed a novel clustering-based algorithm Log3C, which allows you to promptly and precisely identify impactful system problems by utilizing log sequences and key performance indicators (KPIs) of the system. This algorithm was evaluated on real logs collected from the Microsoft online service system, and the results confirmed its effectiveness. However, implementing this approach on a scale of the whole IT infrastructure of a company may be accompanied by scaling problems. Collecting logs from all IT services and then analyzing all these logs can lead to high performance overhead and using this algorithm may not be so effective regarding the computing and storage resources that it needs.

In our work, we implement a solution based on the use of metrics to assess stability and search for vulnerable elements and weak links in the IT infrastructure, which is a distinctive feature of the proposed algorithm. Our algorithm distinguishes the degradation and outage states of the services. This helps us to calculate two more accurate metrics that shows us vulnerable elements of the IT infrastructure that are prone to problems.

Comparative analysis of existing algorithms to calculating stability metrics

A comparative analysis of existing algorithms for calculating IT infrastructure stability metrics needs to be conducted in order to identify their advantages and disadvantages.

Availability [10] is calculated by the formula

$$Availability = 100\% \times \frac{AST - DT}{AST}, \quad (1)$$

where AST is the agreed service time and DT is the sum of downtime. The advantages of this metric include ease of calculation and data collection. However, this metric has a disadvantage: it does not take into account the severity of failures. The severity of a failure means how much it affects the company's production process: slows it down or stops it completely.

Service Level Agreements (SLA) Compliance Ratio [11] is a compliance coefficient for SLA. It is calculated by the formula

$$SLA \text{ Compliance Ratio} = \frac{N_{sla}}{N_{fail}}, \quad (2)$$

where N_{sla} is the number of outages, resolved in compliance with SLA, and N_{fail} is the number of outages. The advantage of this metric is that the resulting number has visual clarity for the client, and therefore inspires confidence. However, the disadvantage of using this metric is the need to document realistic requirements that can be implemented from the very beginning.

Mean Time Between Failures (MTBF) [12] is calculated by the formula

$$MTBF = \frac{T_{el} - T_{dt}}{N_{fail}}, \quad (3)$$

where T_{el} is the total elapsed time, T_{dt} is the total downtime and N_{fail} is the number of failures.

Mean Time To Repair (MTTR) [13] is calculated by the formula

$$MTTR = \frac{T_{main}}{N_{fail}}, \quad (4)$$

where T_{main} is the total maintenance time and N_{fail} is the number of failures.

The advantage of the MTBF and MTTR metrics is that they allow us to understand how well the service will be available in the context of various real-world conditions. However, their disadvantage is that they do not take into account the severity of failures.

First contact resolution rate (FCRR) [14] is calculated by the formula

$$FCRR = \frac{NL_1}{N_{fail}}, \quad (5)$$

where NL_1 is the number of incidents resolved by the first line support and N_{fail} is the number of failures. The advantage of this metric is its convincing economic justification. However, its disadvantage is that this metric depends more on the quality of IT infrastructure support than on its smooth operation.

Based on the comparative analysis given in Table 1, it can be concluded that all metrics have strengths indicated in the “Advantages” column, but none of them can be called optimal and universal, since each of them has their weaknesses indicated in the “Disadvantages” column. Therefore, it is proposed to introduce new metrics for the stability of the IT infrastructure.

Table 1

Comparison between different metrics for calculating stability of the IT-infrastructure

Metric	Formula	Advantages	Disadvantages	Range of possible values
Availability	$\frac{AST - DT}{AST} \times 100$	Ease of calculation and data collection	The severity of failures is not taken into account	From 0% to 100%
SLA Compliance Ratio	$\frac{N_{sla}}{N_{fail}}$	The resulting number has visual clarity for the client	Need to document realistic requirements that can be implemented from the very beginning	From 0 to 1
MTBF	$\frac{T_{el} - T_{dt}}{N_{fail}}$	Allows us to understand how well the service will be available in the context of various real-world conditions	The severity of failures is not taken into account	From 0 seconds to the entire measurement period
MTTR	$\frac{T_{main}}{N_{fail}}$	Allows us to understand how well the service will be available in the context of various real-world conditions	The severity of failures is not taken into account	From 0 seconds to the entire measurement period
FCRR	$\frac{NL_1}{N_{fail}}$	Convincing economic justification	Depends more on the quality of IT infrastructure support than on its smooth operation.	From 0 to 1

Improved stability metrics

To assess the effectiveness of the developed algorithm, it is proposed to introduce two stability metrics: availability and reliability.

Availability is calculated by the formula

$$Availability = 100\% \times \frac{AST - OT}{AST}, \quad (6)$$

where OT is the sum of outage time. Availability describes the extent to which the service can perform its basic functionality.

Reliability is calculated by the formula

$$Reliability = 100\% \times \frac{AST - OT - DT}{AST}, \quad (7)$$

where DT is the sum of degraded time. Reliability describes how much the service is able to perform all its functionality.

The advantage of these metrics is that when they are used together, the severity of failures can be taken into account. They can be calculated based on the data from existing monitoring systems. However, for their correct calculation, it is necessary to separate the outage (OT), and degradation (DT) state of a system.

The range of possible values of the proposed metrics is from 0% to 100%. At the same time, the “reliability” metric can never be greater than the “availability” metric. To reduce the number of calculations performed, the “reliability” metric can be calculated by the formula

$$Reliability = Availability - \frac{DT}{AST} \times 100\% \quad (8)$$

if the value of “availability” metric has already been calculated and the sum of degraded time is also known.

The availability and reliability metrics help us to evaluate the periods of IT-infrastructure stability. However, we need to focus on decreasing the time our infrastructure is instable, so we will also propose two metrics to evaluate instability time. They are called “Service absence” and “Service fragility” and calculated by formulas

$$Absence = 100\% - Availability \quad (9)$$

and

$$Fragility = 100\% - Reliability. \quad (10)$$

Service absence tells us about the percentage of time when the IT infrastructure was completely unavailable and could not be used, which caused resources loss. Service fragility tells us about the percentage of time when the IT infrastructure was either fully unavailable or some non-critical functions of it were broken which caused slowdown of company operations and also caused resources loss. The decreasing of these two metrics will help us understand how much IT downtime was reduced with our algorithm and eventually will give us an understanding of how many resources and production capacities we managed to save.

Proposed algorithm of failure analysis

We propose an algorithm for improving the IT infrastructure stability, and failure analysis is the distinctive feature of it. The “absence” and “fragility” metrics proposed in the paper will be calculated as

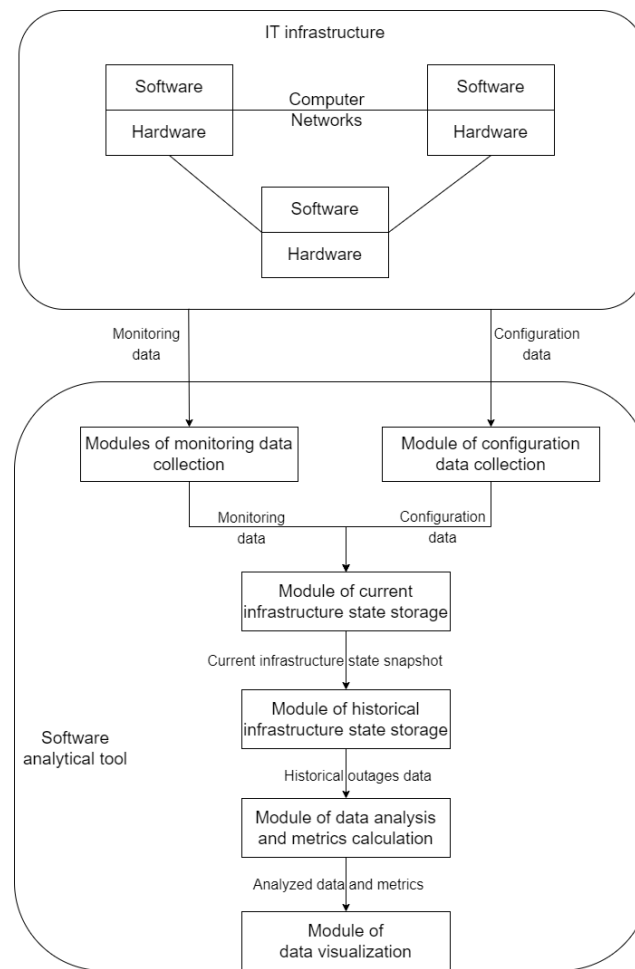


Fig. 1. Proposed algorithm of failure analysis

a part of this algorithm to help us detect the most vulnerable and unstable parts of IT infrastructure. This algorithm is presented in Fig. 1. The top of the figure shows an IT infrastructure consisting of three components: software, hardware and computer networks. The bottom of the figure shows the software analytical tool, which is an essential component of the algorithm. The software analytical tool consists of several modules that work independently.

The algorithm consists in collecting the data about IT infrastructure and passing it through all modules of the software analytical tool as in a pipeline. After the data completes all five stages of the pipeline, we get a visualized information about the most vulnerable components of the IT infrastructure. Each stage of a pipeline is presented by its own module and has its own distinctive features.

The first stage of the pipeline is divided in two parts that work in parallel. The first part is implemented in the modules of monitoring data collection. They are responsible for collecting monitoring data and logs from various distributed components of the IT infrastructure: software, hardware, and computer networks [15], which allows you to get a complete picture of the state of the IT infrastructure. The first part is presented by multiple modules, because each part of IT infrastructure has its own specifics in monitoring data, and a single module cannot collect all logs and metrics from all of IT infrastructure. The second part of the first stage is implemented in the module of configuration data collection. It is responsible for storing internal dependencies of IT infrastructure components on each other. In following stages, this data allows us to find and trace patterns in the behavior of outages, thus more accurately detect the causes of outages and most vulnerable components of IT infrastructure.

The second stage of the pipeline is implemented in the module of current infrastructure state storage. It is responsible for aggregating the data from multiple monitoring data collection modules and configuration data collection module. Such aggregation is implemented using the API [16] and helps us to get a complete understanding of the state of the entire IT infrastructure at a single moment in time. To speed up the module the API allows using “bulk update” request – a single request to update data on all components synchronously.

The third stage of the pipeline is implemented in the module of historical infrastructure state storage. It is responsible for storing the snapshots of connections between the components of the IT infrastructure and their states at each moment of time. This provides us a sufficiently large amount of data for calculating metrics and the ability to analyze previous outages that occurred during the previous years.

The fourth stage of the pipeline is implemented in the module of data analysis and metrics calculation. It is responsible for analyzing IT infrastructure outages, searching for dependencies between these outages and making recommendations to improve stability. This module also provides the calculation of the reliability and availability metrics proposed by us.

The fifth stage is the last stage of the pipeline. It is implemented in the module of data visualization. It is responsible for visualizing the aggregated and analyzed data on the state of IT infrastructure components, the connections between them and calculated metrics. This ensures the visibility of the calculated metrics for the end user, since it is clear where the calculated values came from, and which outages affected them. In addition, the observability of the IT infrastructure is ensured, which allows users to quickly find the source of outages and resolve incidents.

Features of the software implementation

The architecture described above was implemented using a stack of technologies. The software was created as subsystem inside a massive monitoring architecture of an enterprise company, so not all elements of the architecture were created from scratch. Fig. 2 shows the architecture of the implemented software and notes which software components already existed before our implementation, and which were implemented by us.

In particular, monitoring data collection modules were already implemented using Nagios, Zabbix and Solarwinds software products. The log collection module was implemented using the Elasticsearch software product. The IT infrastructure configuration storage module was implemented using the service-now software product.

In the course of the work, the module for storing data on the current health of the IT infrastructure was implemented in a software tool we created, called “Healthcheck DB”. This software tool is written in the Golang language and uses a PostgreSQL database.

The module for storing historical data on the state of the IT infrastructure health was implemented in the course of work by configuring the Prometheus software along with VictoriaMetrics as remote database.

The module of data visualization was implemented in the course of work by configuring the Grafana software. At the same time, the module of data analysis and metrics calculation were implemented using queries from Grafana to Prometheus in Prometheus Query Language (PromQL), and the data visualization module was implemented using dashboards with visualizations [17] of various types in Grafana.

The deployment of all the modules we created was automated. Automation was created in the form of so-called “playbooks” in the configuration management tool Ansible, which allowed us to deploy the software we created on virtual machines with dedicated addresses on the network. At the same time, the software tools themselves work in isolated Docker containers.

In order to secure the collected data, backups of all used databases were created. Backups were implemented as automations in the Jenkins software. These automations are performed once a day, create a backup of each database and save it in the universal artifact repository manager Artifactory.

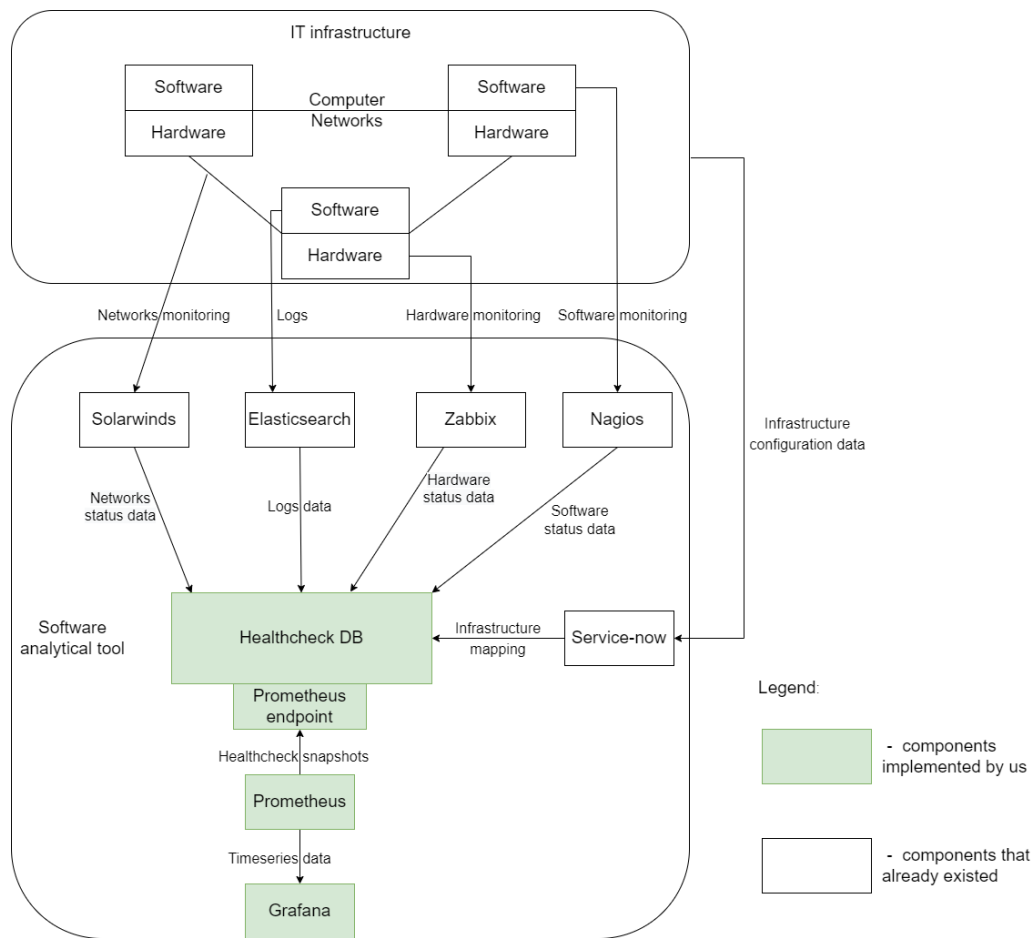


Fig. 2. Architecture of the implemented software

During the entire development process, the Jira software tool [18] was used for task management. To collaborate on code and version control, the GitHub software tool [19] was used. The Visual Studio Code software tool was used as a development environment for writing code. Confluence software was used to store the project documentation.

Description of the dashboards

As a result, several dashboards [17] were created, in order to search for and demonstrate elements of the IT infrastructure that are prone to outages.

Fig. 3 shows a dashboard that demonstrates reliability and availability metrics values for individual hosts of various services for different time intervals in the form of tables. The presented visualization allows you to quickly identify problem periods for each host of services and track the dynamics of changes in metrics in various time intervals: from the last 3 months to the last day. The dashboard also includes filters that allow you to select a list of necessary hosts of services, for example, those used by a certain production team. Thus, it is possible to assess the dynamics of stability of a certain segment of the IT infrastructure.

Fig. 4 shows a dashboard that demonstrates the values of reliability and availability metrics for services as a whole in the form of tables and graphs. The values in the graphs are discrete and are collected with 1 min frequency. The presented visualization allows you to quickly identify problematic periods of services and track the dynamics of changes in availability and reliability in various time intervals: from the last 3 months to the last day. Thus, it is possible to assess the dynamics of the stability of the entire IT infrastructure.

Availability metrics				
Host	Last 90 days	Last 30 days	Last 7 days	Last 24 hours
confluence1.example.com	100%	100%	100%	100%
confluence2.example.com	100%	100%	100%	100%
jira1.example.com	100%	100%	100%	100%
jira2.example.com	100%	100%	100%	100%
jenkins1.example.com	99.874%	99.582%	99.549%	99.814%
Reliability metrics				
Host	Last 90 days	Last 30 days	Last 7 days	Last 24 hours
confluence1.example.com	99.917%	100%	100%	100%
confluence2.example.com	100%	100%	100%	100%
jira1.example.com	99.653%	99.768%	99.356%	100%
jira2.example.com	100%	100%	100%	100%
jenkins1.example.com	97.944%	98.104%	98.156%	98.865%

Fig. 3. Dashboard with availability and reliability metrics for service hosts

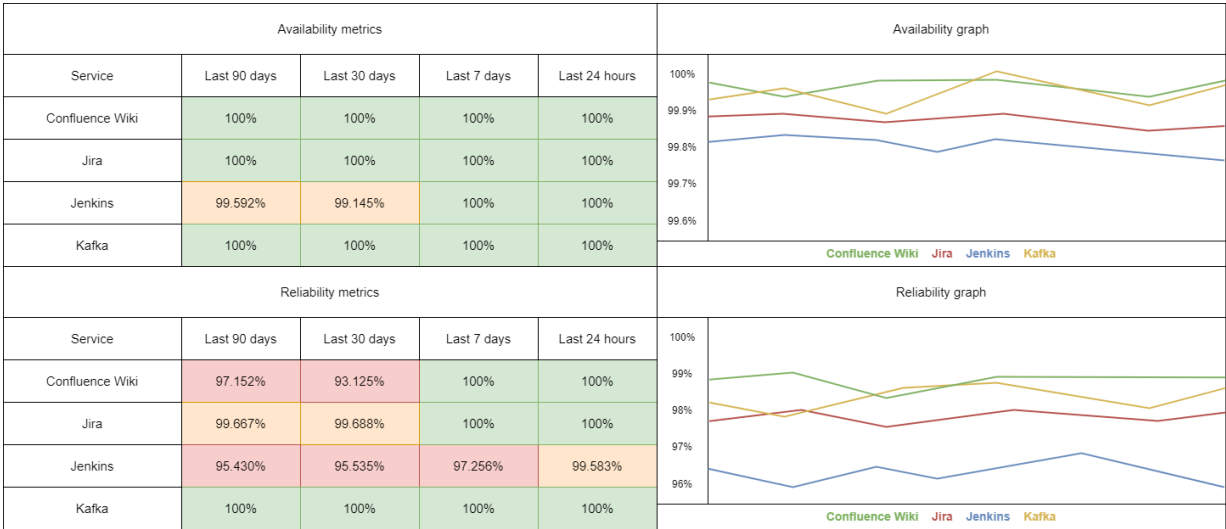


Fig. 4. Dashboard with availability and reliability metrics for services

Fig. 5 shows a dashboard that demonstrates the states of service hosts for a certain period (by default, for the last 24 hours) in the form of a heatmap [20]. On this dashboard, the red highlights the moments of time when service hosts were in the outage state, orange marks the state of degradation and green marks the “correct” state.

The presented visualization allows you to find general trends in service failures. For example, in Fig. 5 there is a simultaneous transition of several hosts of “Jenkins” service into a state of degradation at once, which suggests that these failures had a common cause.

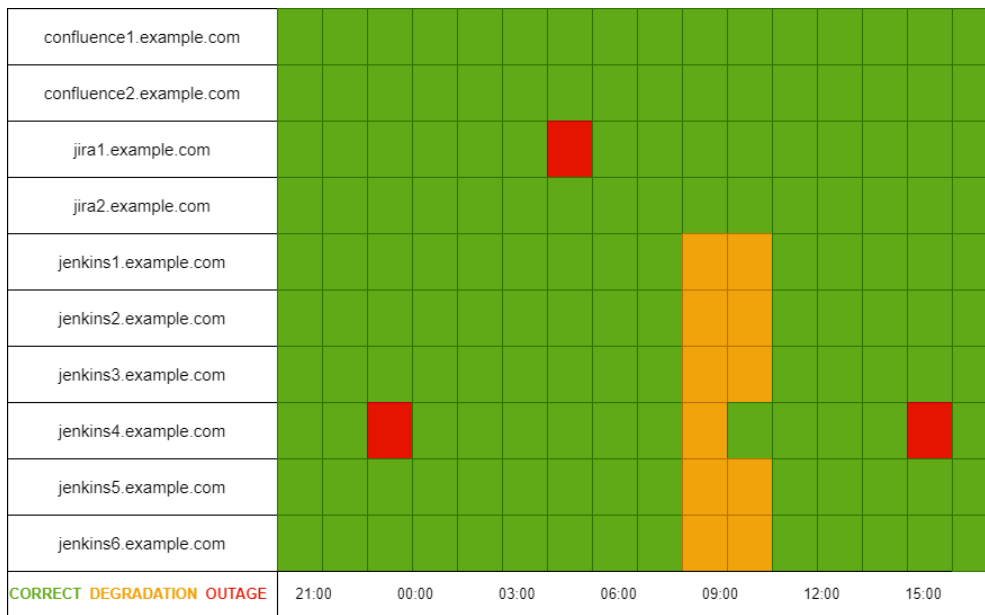


Fig. 5. Dashboard with service hosts states heatmap

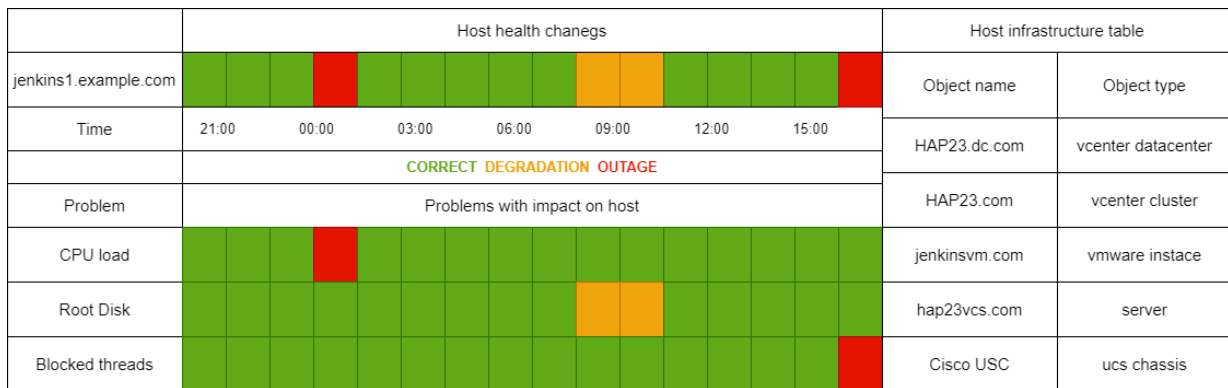


Fig. 6. Dashboard with service host detailed information

Fig. 6 shows a dashboard that provides detailed information about a service host with a list of its infrastructure elements and problems with them. The presented visualization allows you to find the sources of outages and identify vulnerable elements of the IT infrastructure that caused several failures.

Results

The described algorithm to improve the stability of the IT infrastructure was applied in one of the manufacturing companies with more than 10000 employees. Based on the information obtained with the help of the software we created, we managed to get recommendations on improving the stability of one of the services. In particular, one of the found problems was associated with simultaneous daily backups occurring on several hosts at once. The network file system could not cope with a large simultaneous load, which is why the service went into a degradation state.

Changes were applied at the end of January 2022: daily backups on each host started to be performed at different times, which reduced the load on the network file system. Table 2 shows the results of implementing the algorithm in manufacturing company. Prior to our changes, the service stability indicators

for January 2022 were as follows: availability 98.50%, reliability 92.58%. After the implementation of the developed software, the service stability indicators for February were as follows: availability 98.69%, reliability 94.43%.

Table 2

Results of implementing the algorithm in manufacturing IT-company

Metric	January 2022	February 2022	Relative change
Availability	98,50%	98,69%	0,19%
Reliability	92,58%	94,43%	2,00%
Absence	1,50%	1,31%	-12,67%
Fragility	7,42%	5,57%	-24,93%

Such an increase in metrics is a significant achievement, since even tenths and hundredths of a percent are important when agreeing on SLAs [21]. There are results that are even more impressive if we turn to the relative change of absence and fragility metrics. We managed to reduce the absence periods by 13% and fragility periods by 25% relative to the same values in the previous month. This shows a significant decrease of time during which the material and human resources of the company were idle.

Conclusion

In the course of the work, an algorithm was proposed to improve the stability of the IT infrastructure, based on the collection and analysis of data on its status. The proposed algorithm is based on two new metrics: availability and reliability, which were created based on a comprehensive study and comparative analysis of existing stability metrics. A distinctive feature of the new metrics is that they take into account the severity of failures in the system. The proposed software architecture of the system and its implementation in the software tool responsible for monitoring the stability of IT services made it possible to detect vulnerable elements of the IT infrastructure in an enterprise manufacturing company. After eliminating the vulnerabilities found, the relative decrease of instability periods was recorded using two metrics at once: the absence time of the service decreased by 13%, and the fragility time decreased by 25%. Such significant decrease of time during which the material and human resources of the company were idle shows the effectiveness of the developed algorithm.

REFERENCES

1. **Drobintsev P.D., Kotlyarova L.P., Voinov N.V., Tolstoles A.A., Maslakov A.P., Krustaleva I.N.** Automating preparation of small-scale production for reliable net-centric IoT workshop. CEUR Workshop Proceedings: APSSE 2019, 2019, pp. 75–85.
2. **Lazareva N.B.** Organizatsiia otkazoustoichivogo (HA) klastera [Organization of high-availability (HA) cluster]. E-Scio.ru, 2021, no. 2 (53), pp. 61–66.
3. **Unagayev S.** Organizatsiia IT-infrastruktury kompanii [Organization of IT-infrastructure in a company]. Sistemnyi administrator [System administrator], 2013, no. 4 (125), pp. 40–41.
4. **Autenrieth P., Lörcher C., Pfeiffer C., Winkens T., Martin L.** Current Significance of IT-Infrastructure Enabling Industry 4.0 in Large Companies. 2018 IEEE International Conference on Engineering, Technology and Innovation (ICE/ITMC), 2018, pp. 1–8. DOI: 10.1109/ICE.2018.8436244
5. **Wang G., Zhang W., Huang C., Chen Z.** Service Availability Monitoring and Measurement Based on Customer Perception. 2018 IEEE 9th International Conference on Software Engineering and Service Science (ICSESS), 2018, pp. 328–331. DOI: 10.1109/ICSESS.2018.8663889

6. **Ahmad A., Ngah L., Ibrahim I.** A Review of Service Quality Elements towards the Overlapping IT Framework Process on the IT Hardware Support Services (ITHS). *International Journal of Advanced Trends in Computer Science and Engineering*, 2020, Vol. 9, no. 1.4, pp. 423–432. DOI: 10.30534/ijatcse/2020/6091.42020
7. **Pan C., Xu H., Li W., Tu Z., Xu X., Wang Z.** Quality Monitoring and Measuring for Internet of Services. 2021 International Conference on Service Science (ICSS), 2021, pp. 107–114. DOI: 10.1109/ICSS53362.2021.00025
8. **Alimi O.A., Ouahada K., Abu-Mahfouz A.M.** A Review of Machine Learning Approaches to Power System Security and Stability. *IEEE Access*, 2020, vol. 8, pp. 113512–113531. DOI: 10.1109/ACCESS.2020.3003568
9. **He S., Lin Q., Lou J., Zhang H., Lyu M., Zhang D.** Identifying impactful service system problems via log analysis. *ESEC/FSE 2018: Proceedings of the 2018 26th ACM Joint Meeting on European Software Engineering Conference and Symposium on the Foundations of Software Engineering*, 2018, pp. 60–70. DOI: 10.1145/3236024.3236083
10. **Bukhsh M., Abdullah S., Bajwa I.S.** A Decentralized Edge Computing Latency-Aware Task Management Method With High Availability for IoT Applications. *IEEE Access*, 2021, vol. 9, pp. 138994–139008. DOI: 10.1109/ACCESS.2021.3116717
11. **Li L., Dong J., Zuo D., Wu J.** SLA-Aware and Energy-Efficient VM Consolidation in Cloud Data Centers Using Robust Linear Regression Prediction Model. *IEEE Access*, 2019, vol. 7, pp. 9490–9500. DOI: 10.1109/ACCESS.2019.2891567
12. **Jiang C., Wang H., Yang Y., Fu Y.** Construction and Simulation of Failure Distribution Model for Cycloidal Gears Grinding Machine. *IEEE Access*, 2022, vol. 10, pp. 65126–65140. DOI: 10.1109/ACCESS.2022.3184318
13. **Li A., Han G., Ohtsuki T.** Multiple Radios for Fast Rendezvous in Heterogeneous Cognitive Radio Networks. *IEEE Access*, 2019, vol. 7, pp. 37342–37359. DOI: 10.1109/ACCESS.2019.2904942
14. **Al-Akwaa N.** The application of Lean Six Sigma principles in the technical support call center: First contact resolution. USA: California State University, Dominguez Hills, 2015. 144 p.
15. **Rukavitsyn A.N.** Data clustering in distributed monitoring systems. *Informatsionno-upravliaiushchie sistemy [Information and Control Systems]*, 2019, no. 2, pp. 35–43. DOI: 10.31799/1684-8853-2019-2-35-43
16. **Huang Q., Xia X., Xing Z., Lo D., Wang X.** API Method Recommendation without Worrying about the Task-API Knowledge Gap. 2018 33rd IEEE/ACM International Conference on Automated Software Engineering (ASE), 2018, pp. 293–304. DOI: 10.1145/3238147.3238191
17. **Vázquez-Ingelmo A., García-Peñalvo F.J., Therón R.** Information Dashboards and Tailoring Capabilities – A Systematic Literature Review. *IEEE Access*, 2019, vol. 7, pp. 109673–109688. DOI: 10.1109/ACCESS.2019.2933472
18. **Kovalev A.D., Voinov N.V., Nikiforov I.V.** Using the Doc2Vec Algorithm to Detect Semantically Similar Jira Issues in the Process of Resolving Customer Requests. *Studies in Computational Intelligence*, 2020, Vol. 868, pp. 96–101. DOI 10.1007/978-3-030-32258-8_11
19. **Voinov N., Rodriguez Garzon K., Nikiforov I., Drobintsev P.** Big data processing system for analysis of GitHub events. *Proceedings of 2019 22nd International Conference on Soft Computing and Measurements (SCM 2019)*, 2019, pp. 187–190. DOI: 10.1109/SCM.2019.8903782
20. **Perrot A., Bourqui R., Hanusse N., Auber D.** HeatPipe: High Throughput, Low Latency Big Data Heatmap with Spark Streaming. 2017 21st International Conference Information Visualisation (IV), 2017, pp. 66–71. DOI: 10.1109/iV.2017.45
21. **Zharinova O.V.** Improving the efficiency of IT infrastructure management using ITIL. *StudNet*, 2021, vol. 4, no. 2, p. 43.

INFORMATION ABOUT AUTHORS / СВЕДЕНИЯ ОБ АВТОРАХ

Varlamov Dmitrii A.

Варламов Дмитрий Андреевич

E-mail: varlamov_dmitry99@mail.ru

Nikiforov Igor V.

Никифоров Игорь Валерьевич

E-mail: igor.nikiforovv@gmail.com

ORCID: <https://orcid.org/0000-0003-0198-1886>

Ustinov Sergey M.

Устинов Сергей Михайлович

E-mail: usm50@yandex.ru

ORCID: <https://orcid.org/0000-0003-4088-4798>

Submitted: 03.06.2024; Approved: 24.07.2024; Accepted: 30.07.2024.

Поступила: 03.06.2024; Одобрена: 24.07.2024; Принята: 30.07.2024.

Computer Simulations of Telecommunication, Control, and Social Systems

Моделирование вычислительных, телекоммуникационных, управляющих и социально-экономических систем

Research article

DOI: <https://doi.org/10.18721/JCSTCS.17204>

UDC 517.938:070



A MATHEMATICAL MODEL OF INFORMATION CONFRONTATION: DISCRETE ADAPTIVE CONTROL OF THE SYSTEM

S.V. Timofeev ✉, *A.V. Baenkhayeva*

Baikal State University, Irkutsk, Russian Federation

✉ timofeevsv12@gmail.com

Abstract. This article presents initial results of controlling a mathematical model of information confrontation, proposed by the authors in earlier works. The model is a system of ordinary differential equations with quadratic nonlinearity on the right side. The introduction defines the novelty of the approach and outlines the differences from previously used ones. Additionally, the substantive meaning of the variables and parameters of the system is described, and the stages of research on this model are briefly presented. In the parameter space, a component is established, by controlling which we obtain relations that determine the predictable behavior of the system trajectory from any initial point corresponding to the substantive meaning. In the main part of the work, an algorithm for constructing discrete adaptive control is proposed, which allows reducing the information confrontation to a scenario advantageous for one of the parties. The example shows the procedure for using the model and the algorithm for building the control step-by-step. The numerical solution of the system of differential equations was performed using the `solve_ivp` module for solving ordinary differential equations of the SciPy library of the Python programming language.

Keywords: mathematical model, information confrontation, information promotion, differential equation, adaptive control, numerical solution of differential equation system

Citation: Timofeev S.V., Baenkhayeva A.V. A mathematical model of information confrontation: discrete adaptive control of the system. *Computing, Telecommunications and Control*, 2024, Vol. 17, No. 2, Pp. 38–51. DOI: [10.18721/JCSTCS.17204](https://doi.org/10.18721/JCSTCS.17204)

Научная статья

DOI: <https://doi.org/10.18721/JCSTCS.17204>

УДК 517.938:070



МАТЕМАТИЧЕСКАЯ МОДЕЛЬ ИНФОРМАЦИОННОГО ПРОТИВОБОРСТВА: ДИСКРЕТНОЕ АДАПТИВНОЕ УПРАВЛЕНИЕ СИСТЕМОЙ

С.В. Тимофеев  , *А.В. Баенхаева*Байкальский государственный университет,
г. Иркутск, Российская Федерация timofeevsv12@gmail.com

Аннотация. В статье представлены первые результаты управления математической моделью информационного противоборства, предложенной авторами в более ранних работах. Модель представляет собой систему обыкновенных дифференциальных уравнений с квадратичной нелинейностью в правой части. Во введении определена новизна подхода и его отличие от ранее использовавшихся. Также описан содержательный смысл переменных и параметров системы и кратко представлены этапы исследования данной модели. В пространстве параметров установлена компонента, управляя которой, можно получить соотношения, определяющие предсказуемое поведение траектории системы из любой начальной точки, соответствующей содержательному смыслу. В основной части работы предложен алгоритм построения дискретного адаптивного управления, который позволяет свести информационное противоборство к выгодному для одной из сторон сценарию. На примере показана процедура использования модели и алгоритма построения управления по шагам. Численное решение системы дифференциальных уравнений проводилось с использованием модуля `solve_ivp` для решения обыкновенных дифференциальных уравнений библиотеки SciPy языка программирования Python.

Ключевые слова: математическая модель, информационное противоборство, продвижение информации, дифференциальное уравнение, адаптивное управление, численное решение системы дифференциальных уравнений

Для цитирования: Timofeev S.V., Baenkhaeva A.V. A mathematical model of information confrontation: discrete adaptive control of the system // Computing, Telecommunications and Control. 2024. Т. 17, № 2. С. 38–51. DOI: 10.18721/JCSTCS.17204

Introduction

Interest in modeling the process of promoting new information through the media is determined by the fact that this information can be used with equal success both to unite and stabilize society, and to divide and destabilize it. Success in promoting fundamentally new ideas into society largely depends on the positions of the main acting forces. On the one hand, influential media with the ability to shape public opinion, and, on the other hand, various subjects of society such as expert communities, executive authorities, political parties, public organizations have the ability to use another part of the media to present alternative point of view and «promotion» of their concepts within the society [1]. Here we are dealing with a certain information confrontation.

A number of noteworthy works are dedicated to modeling this process. In article [2] a detailed review of some of them was conducted. It was observed that they share a common approach to modeling the process of information confrontation. All models are described through characteristics of the population of various recipient groups, which, in one way or another, belong to one of the conflicting parties in the information space [3–10]. In the future, it is likely that confirmation of the adequacy of each of the obtained theoretical models by empirical data will be required, which will require the use of standard sociological tools

in the form of a survey of a sample population, followed by the use of traditional statistical methods for parameter identification and data analysis.

However, researchers now have new tools for their investigative work, such as Data Science and Text Mining. New opportunities have also opened up. We have proposed a fundamentally different approach to analyzing the spread of new information through the media, which does not rely on sampling theory to study public opinion, but instead involves working with big data. Sociologists studying public opinion argue that the inherent characteristics of Big Data provide more effective forecasting capabilities than traditional methods [11, 12]. The absence of samples ($n=All$) and direct work with statistical populations or very large portions of them, data scalability, constant automated collection of data in archives and the ability to quickly process them ultimately lead to high reliability and demand for “real-time” forecasting. Therefore, in our opinion, it is more relevant in modern conditions to conduct research not by measuring the number of people taking a position “for” or “against” a certain point of view, but by analyzing the volume and intensity of information received in the media aimed at achieving goals that do not coincide in interests.

This work serves as a continuation of a systematic study of the mathematical model of information confrontation that accompanies the stages of emergence and dissemination of information through the media, aimed at promoting new views or concepts in society.

$$\begin{aligned}
 \frac{dN}{dt} &= \beta N - \gamma AN, \\
 \frac{dC}{dt} &= \alpha AN - \mu(C - C_*), \\
 \frac{dA}{dt} &= \rho C - \eta \gamma AN - \lambda A, \\
 \frac{di}{dt} &= \sigma N - \omega i.
 \end{aligned}
 \tag{1}$$

The phase variables of this system are quantities identified as factors that describe the most general patterns of confrontation in the dissemination of information through the media:

$N(t)$ is a quantitative characteristic of the volume of news information (quantity of articles, messages of various types, units ($quan\{N\}$)), corresponding to the promotion in the information space of new – reformist, sometimes overly radical – views;

$C(t)$ is the number of entities in the structure of the information space with special resources, the purpose of which is to preserve previously accepted concepts in society (ideological or technological, units ($quan\{C\}$));

$A(t)$ is a quantitative characteristic of the volume of conservative information (quantity of articles, messages of various types, units ($quan\{A\}$)), opposed to the spread of radical views in the information space;

$i(t)$ is an indicator of the share of the population that is loyal to new ideas appearing in the media:
 $i = 1 - \frac{I^*}{I}$, where $I(\%)$ corresponds to the full acceptance of prevailing conditions in society before the start of observations; $I^*(\%)$ is the corresponding characteristic of the acceptance of these positions when disseminating new perspectives in the media. The content characteristics of the model parameters are presented in Table 1.

In the system (1), the variable $i(t)$ appears only in the last equation, so the study was carried out for a lower-dimensional system, rewritten in a more convenient for study form:

Table 1

Content characteristics of the model parameters [18]

$\beta \geq 0$	An indicator characterizing the intensity of spread of new information through the media $\left(\frac{1}{t}\right)$.
$\gamma \geq 0$	An indicator characterizing the possibility of neutralizing the effect of information that appears after presenting an alternative opinion $\left(\frac{1}{\text{quan}\{A\} \cdot t}\right)$. Inversely proportional to the amount of information A per unit of time.
$\alpha \geq 0$	An indicator characterizing the intensity of societal reaction to the confrontation of alternative points of views $\left(\frac{\text{quan}\{C\}}{\text{quan}\{A\} \cdot \text{quan}\{N\} \cdot t}\right)$. Average number of conservative media outlets, which contrasts with the volume of new trend messages over a given period of time.
$\mu > 0$	A coefficient inversely proportional to the time of operation of additionally created agencies of information $\left(\frac{1}{t}\right)$.
C_*	An amount of information resource for daily support of the currently prevalent concept of society.
$\rho \geq 0$	An average speed of news appearance from one information entity $C \left(\frac{\text{quan}\{A\}}{\text{quan}\{C\} \cdot t}\right)$.
$\eta \geq 0$	An average percentage of information A directed to neutralize the effect of messages N.
$\lambda > 0$	A coefficient inversely proportional to the time of forgetting information $A \left(\frac{1}{t}\right)$.
$\sigma \geq 0$	An indicator characterizing the pace of adopting new idea that have appeared in the media $\left(\frac{1}{\text{quan}\{N\} \cdot t}\right)$.
$\omega \geq 0$	An indicator characterizing the return, due to the inertia of thinking, to the existing concept of society $\left(\frac{1}{t}\right)$.

$$\begin{aligned}
 \frac{dC}{dt} &= \alpha AN - \mu(C - C_*), \\
 \frac{dA}{dt} &= \rho C - (\lambda + \eta\gamma N) A, \\
 \frac{dN}{dt} &= (\beta - \gamma A) N,
 \end{aligned}
 \tag{2}$$

with initial conditions, due to its autonomy:

$$C(0) = C_0 \geq 0, \quad A(0) = A_0 \geq 0, \quad N(0) = N_0 \geq 0.
 \tag{3}$$

Articles [13–15] describe in detail the stages and results of the theoretical part of the modeling process [16, 17]. Therefore, in the work [13], the mathematical formulation of the problem was carried out and a mathematical model was built. The correctness of the model was checked, including dimensional control, nature of dependencies, physical relevance and existence of solutions. Several important regions were identified in the parameter space of the model, where the dynamic system exhibits different

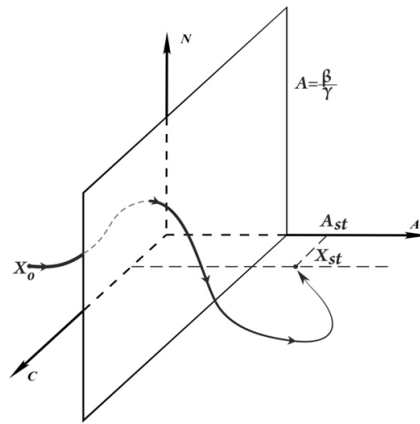


Fig. 1. Qualitative behavior of the trajectory
of the system (2) from the point $X_0 = (C_0; A_0; N_0) = (10; 12; 68)$ [18]

topological properties. In articles [13, 14], based on the Lyapunov function method, qualitative analysis of solution behavior was conducted in each parameter region, and global phase portraits of trajectories of the proposed dynamic system were built. A detailed interpretation of the model under study was carried out in [15].

In article [18], the first step of the next stage of modeling was taken – checking the adequacy of the model or assessing the correspondence of the model to real data. The model performed well in the analysis of one of the high-profile information events at the beginning of 2022 – media coverage of the attempted coup in Kazakhstan. A comparison of the qualitative behavior of the integral curves of the model and graphs presented by the media monitoring system during the period of observation of the event showed good consistency. Fig. 1 shows the calculated trajectory of the system (2), which accurately reflects the real situation. As can be seen from the figure, an increase in the values of $N(t)$ and $A(t)$ of the trajectory $X(t) = (C(t), A(t), N(t))$ after the start of movement (the point $X_0 = (C_0; A_0; N_0) = (10; 12; 68)$ was obtained using the media monitoring system) indicates a confrontation between different points of view when covering the event. The result shows the outcome of this confrontation (Fig. 1).

$X_{st} = (C_{st}, A_{st}, N_{st}) = \left(C_*, \frac{\rho C_*}{\lambda}, 0 \right)$ is an asymptotically stable stationary solution interpreted as a state of society in which a certain concept dominates, and to support it, an administrative resource in the amount of C_* uses a sufficient amount of information, from its point of view, in the media $\frac{\rho C_*}{\lambda}$.

This step is important in the sense that a “sample” of the trajectory of the system (2–3) was obtained, which can be interpreted as a successful outcome of information confrontation for those entities defending the accepted societal views against unwanted perspectives covered in the media.

However, such a trajectory behavior determined by a set of parameters corresponds to only one of the many scenarios described in [15], namely: when performing inequalities

$$\begin{cases} \gamma \rho C_* > \lambda \beta \\ \rho \alpha > \mu \eta \gamma + \beta \eta \gamma \end{cases} \quad (4)$$

any trajectory of the system (2) starting from an arbitrary point in the set $R_+^3 = \{(C, A, N) \in R^3 : C \geq 0, A \geq 0, N \geq 0\}$ tends towards an asymptotically stable stationary solution $X_{st} = (C_{st}, A_{st}, N_{st}) = \left(C_*, \frac{\rho C_*}{\lambda}, 0 \right)$.

In other cases, depending on the parameter relations and initial conditions trajectory behavior may significantly differ [15] from that presented in the figure. In such cases, phase portraits describing the system's dynamics will have different topological properties [19]. Thus, for a favorable – in terms of substantive meaning – outcome of the confrontation, interested parties need to manage the dynamic model of the ongoing process. This, for example, will help approximate the trajectory of the system to a “sample” and, therefore, from the perspective of the conservatively inclined part of society, ensure the desired outcome in the struggle against undesirable information in the media space. *This work specifically considers this case.*

The system (2) describing the process of information confrontation can be considered as controlled, understanding control as an influence on certain parameters of the system. In this case, based on the system of inequalities (4), it is logical to assume that the parameter ρ of the system (2) is most suitable for control. Indeed, by increasing it, considering the substantive meaning and leaving other parameters unchanged, under certain conditions, it is possible to achieve the satisfaction of inequalities (4).

Formulation of the problem

Let us assume that active discussions of an extraordinary event have started on media channels capable of influencing certain values established in society. Within the framework of the research object, it is necessary to formulate a thesis that describes the existing societal concept. In accordance with this, all information supporting this thesis will reflect the quantitative characteristic of the phase variable $A(t)$. We will refer to it as information with a positive or optimistic tone. Consequently, any information contradicting this thesis in any form will reflect the quantitative characteristic of the phase variable $N(t)$ and have a negative or pessimistic tone. Informational bodies publishing information with a positive tone, collectively, will reflect the quantitative characteristic of the phase variable $C(t)$. Thus, by using electronic media monitoring systems and the algorithm described in [18], initial conditions (3) of the system (2) describing the movement of information flows directed at covering this event can be determined.

Let us denote the beginning of the trajectory movement of the system at $t = 0$ as a point $X^* = (C^*; A^*; N^*)$ in the phase space of the system (2). For example, when covering the aforementioned attempted coup in Kazakhstan by the media, the value of the variable N^* can be determined based on information about the initial occurrences of negative reports (see Table 2).

Table 2

Number of negative messages by day during January [18]

Day of the month	1	2	3	4	5	6	7	8	9	10	11	12	13	14	15	16
Number of negative messages	1	0	1	0	68	327	177	127	94	362	151	110	91	85	58	41
Day of the month	17	18	19	20	21	22	23	24	25	26	27	28	29	30	31	
Number of negative messages	50	52	38	37	14	13	8	20	6	14	96	47	14	17	8	

According to these data, $N^* = 68$. The value of $A^* = 12$ was taken as the arithmetic mean of the number of positive reports several days before the appearance of negative reports (see Table 3).

To determine the initial condition $C^* = 10$, it was necessary to use data on permanent sources providing the media with positive information about the CSTO for the entire previous year (see Fig. 2).

Let us assume that after some time values of all parameters of this system have been determined.

It should be noted that when analyzing the media coverage of the events in Kazakhstan, the possible range of variation for each parameter was determined to calculate their values. Subsequently, using the well-known Monte Carlo method, a set of parameters was chosen that provided the most acceptable deviation of the calculated trajectory from the actual monitoring data. The complete algorithm for parameter calculation is planned to be described in the next paper. For example, when estimating the parameter

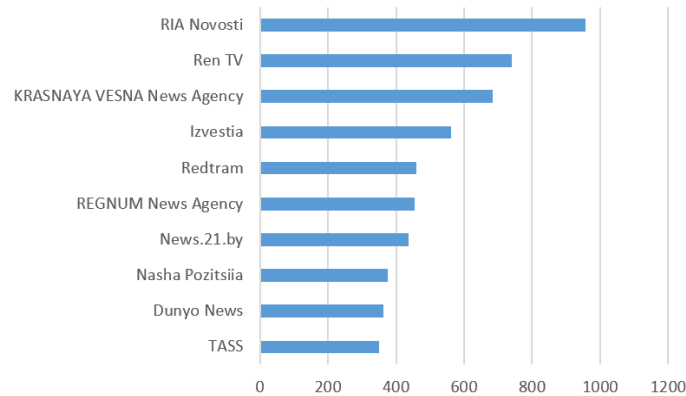


Fig. 2. Top sources with positive information A about the CSTO for 2021 [18]

β , a differential equation $\frac{dN}{dt} = \beta N$ was used, derived from system (2) after removing the nonlinear term from the right side of the corresponding equation. Taking into account the initial conditions, its solution has the form: $N(t) = 68 \exp(\beta t)$. According to Table 2, $N(1) = 327$, which is possible with $\beta_{\min} = 1,57$. Further comparison of parameter values showed that $\beta = 1.9$ most accurately reflects the situation. A similar analysis allowed estimation of the parameters ρ and α . To estimate the parameter λ , data from experiments on memory studies were used, based on which the Ebbinghaus's forgetting curve was constructed¹, showing how the level of retention of learned information logarithmically decreases over time. The range of γ and η values was determined according to the monitoring system data based on text sentiment analysis. In particular, using the built-in rating scale, the analysis showed that the messages A were mostly aimed not at neutralizing the messages N , but rather at proving the usefulness of the creation of the CSTO and the need to use this organization's armed forces in these conditions. Finally, the value of μ was determined based on data about the emergence of information from new sources that had not previously shown interest in the topic.

Table 3

Number of positive messages by day during January [18]

Day of the month	1	2	3	4	5	6	7	8	9	10	11	12	13	14	15	16
Number of negative messages	22	5	8	13	272	3653	2896	1933	1474	2797	1871	1282	1499	817	718	481
Day of the month	17	18	19	20	21	22	23	24	25	26	27	28	29	30	31	
Number of negative messages	349	360	500	206	141	158	94	92	123	82	91	120	158	51	90	

If the value of the parameter is such that the system of inequalities (4) is satisfied, then a successful outcome of information confrontation for the control authorities is guaranteed. Otherwise, as shown in [15], scenarios of information confrontation may have different results. Therefore, for a successful outcome, it is necessary to adjust the parameter ρ through adaptive control $u = u(t)$ [20]. Let a control

¹ Averell, L., Heathcote, A. The shape of the forgetting curve and the fate of memories. *Journal of Mathematical Psychology*, 2011, Vol. 55, no. 1, pp. 25–35.

function $u = u(t)$ be given characterizing the level of increase in the parameter ρ of system (2) and satisfying constraints:

$$0 \leq u(t) \leq u_{\max}, \quad 0 \leq t \leq T, \quad (5)$$

where $u_{\max} \geq 0$ is the maximum degree of increase in the average speed of news appearance from one information entity ρ (according to the semantic characteristic of the parameter), T is the time interval of observing the information event. Let us assume that under the control influence, the parameter ρ of the system (2) can change from the value ρ_0 to $\rho_{\max} = \rho_0(1 + u_{\max})$, where ρ_0 is the value of the parameter set during identification, taking into account media monitoring at the initial stage, and u_{\max} is such an arbitrary value that the parameter ratios satisfy the inequalities (4).

The system (2) with the introduced values will have the following form:

$$\begin{aligned} \frac{dC}{dt} &= \alpha AN - \mu(C - C_*), \\ \frac{dA}{dt} &= \rho(1 + u)C - (\lambda + \eta\gamma N)A, \\ \frac{dN}{dt} &= (\beta - \gamma A)N. \end{aligned} \quad (6)$$

The control objective may be to ensure that the trajectory behavior of the system is close to a “sample”, i.e., asymptotically approaching the point $X = \left(C_*, \frac{\rho C_*}{\lambda}, 0 \right)$. In the proposed model, such an outcome is primarily associated with the dynamics of the volume of news information $N(t)$. Therefore, as a “sample” for control, we find the solution of the system (6) at $u \equiv u_{\max}$ with the initial condition $C(0) = C_*$, $A(0) = A^*$, $N(0) = N^*$ and extract the integral curve $N^*(t)$. To define the control criterion for the considered process on the interval $[0; T]$, we set up a uniform grid:

$$\Xi = \left\{ t_i : t_i = i\Delta t, \quad i = \overline{1, M}; \quad \Delta t = \frac{T}{M} \right\}, \quad (7)$$

on which we fix the volume of news information corresponding to the “sample”:

$$N^*(t_i) = N_i^*, \quad i = \overline{1, M}. \quad (8)$$

We will consider that for the solution of system (6), the condition:

$$\left| N(u(t), t_1) - N_i^* \right| < \varepsilon, \quad i \in I = \{r, \dots, M\}, \quad 1 < k \leq r < M, \quad (9)$$

with a sufficiently small ε corresponds to achieving a successful outcome of information confrontation. Here, $k: t_{k-1}$ is the moment of the start of control, before which it is assumed to identify the parameters of the system (2) and, accordingly, (6). We will call the condition (9) the criterion of discrete adaptive control for the system (6).

Thus, the stated problem involves constructing the control $u(t)$, $t \in [0; T]$, that ensures the fulfillment of condition (9) for the solution of the system (6) with initial conditions (3) under the constraint (5).

Algorithm for adaptive control construction

Let us define the set U as follows. Let us assume that on each interval $[t_{i-1}; t_i]$, $i = \overline{1, M}$ the function $u(t)$ is constant and satisfies the inequalities (5). Thus, the control function will be chosen from the set of piecewise-constant functions on the interval $[0; T]$. Consequently,

$$U = \left\{ u(t) : u(t) = u_{i-1} \in [0; u_{\max}], t \in [t_{i-1}; t_i], i = \overline{1, M}, u(T) = u_{M-1} \right\}.$$

We will assume that under every admissible control $u = u(t)$ the system (6) with initial conditions (3) has a unique solution $X(u(t), t) = (C(u(t), t), A(u(t), t), N(u(t), t))$, $u(t) \in U$, defined for all $t \in [0; T]$.

According to the criterion (9) it is required to construct control $u(t) \in U$ satisfying the condition:

$$|N(u_{i-1}, t_i) - N_i^*| < \varepsilon, \quad i \in I.$$

To construct the control function $u(t) \in U$, the following algorithm is proposed:

Reduce the problem solution to the sequential integration of the system (6) on intervals $t \in [t_{i-1}; t_i]$, $i = \overline{1, M}$. Thus, only phase variables are unknown functions at each fixed value u_{i-1} . Their right end values are the initial conditions for the next time interval. Let us assume that $u_0 = u_1 = \dots = u_{k-2} = 0$. On intervals $[t_{i-1}; t_i]$, $i \geq k$, denote

$$\Psi(u_{i-1}) = N(u_{i-1}, t_i) - N_i^*,$$

where $N(u_{i-1}, t_i)$ is the value of the function $N(u(t), t)$ at the point t_i for a fixed u_{i-1} . The set (8) is defined in such a way that $N_i^* < N(0, t_i)$, $i \in I$, i.e., $\Psi(0) > 0$, $i \in I$. The following options are possible:

- If $N_i^* \leq N(u_{\max}, t_i) < N(0, t_i)$, $i \in I$, then fix $u_{i-1} = u_{\max}$;
- If $N(u_{\max}, t_i) < N_i^* < N(0, t_i)$, $i \in I$, then to find u_{i-1} as solving the nonlinear equation

$$\Psi(u_{i-1}) = 0, \quad u_{i-1} \in [0; u_{\max}]. \quad (10)$$

Due to the continuous dependence of the system (2) on parameters and the fact that $\Psi(0) > 0$, and $\Psi(u_{\max}) < 0$, the bisection method, for example, can be applied to solve equation (10).

Thus, it seems possible to determine all continuous components of the control function $u(t)$ and, consequently, solve the stated problem. Then the control function can be represented as follows:

$$u(t) = u_0 + \sum_{k=1}^{M-1} \theta(t - t_{k-1})(u_k - u_{k-1}), \quad (11)$$

where $\theta(t)$ is the Heaviside's function, defined by the formula

$$\theta(t) = \begin{cases} 1, & t \geq 0, \\ 0, & t < 0. \end{cases}$$

Numerical solution of the adaptive control problem

Numerical integration of the system (6) was performed using the solve_ivp module of the SciPy library in the Python programming language. The solve_ivp module provides a powerful tool for solving systems of differential equations in modeling and researching various processes [21].

As part of the SciPy library, the solve_ivp module seamlessly integrates with other modules and tools, such as NumPy and Matplotlib, offering a choice of several numerical methods for solving complex ODE systems [22]. One notable feature of the solve_ivp function is that it returns an array of numerical solution values at each point from the time array [23].

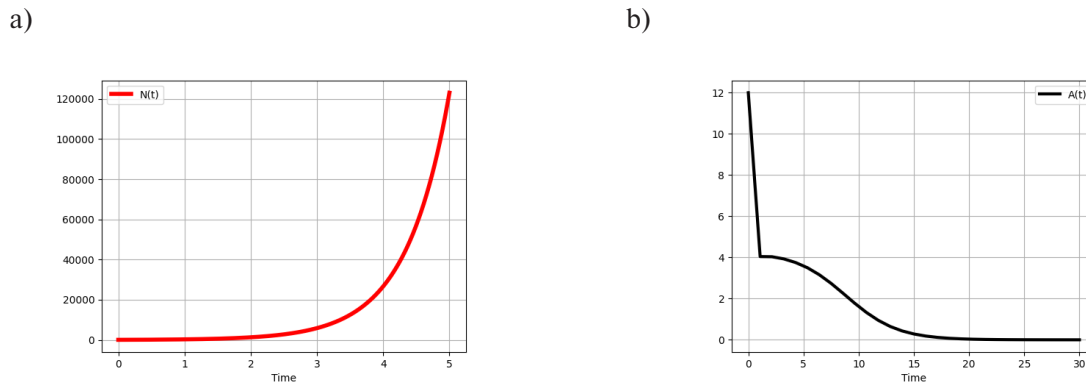


Fig. 3. Integral curves a) $N(t)$, and b) $A(t)$ of the system (2) with initial conditions $C(0) = 10$, $A(0) = 12$, $N(0) = 68$ and parameter values $\beta = 1,9$; $\gamma = 0,1$; $\alpha = 0,09$; $C_* = 10$; $\mu = 0,3$; $\rho = 5$; $\eta = 2,54$; $\lambda = 1/3$

To build adaptive control let us consider the situation described in [18]. When imitating different scenarios, it was noticed that numerical integration of the system (2) with initial conditions $C(0) = 10$, $A(0) = 12$, $N(0) = 68$ and parameter values

$$\beta = 1,9; \gamma = 0,1; \alpha = 0,09; C_* = 10; \mu = 0,3; \rho = 5; \eta = 2,54; \lambda = 1/3, \quad (12)$$

which are located outside near the boundary of the domain (4), the behavior of the system's solution changes abruptly.

The dynamics of variables $N(t)$ and $A(t)$ in this case have the following representation (Fig. 3).

For these parameter values the value of the phase variable is $N(t) \rightarrow +\infty$ when $t \rightarrow +\infty$. From a substantive point of view, this corresponds to a situation where the appearance in the media of information aimed at changing society's concept can find support and lead to an undesirable threat to the traditional system of views for government structures. In this regard, it is necessary to determine methods of control that allow changing the dynamics of factors $N(t)$ and $A(t)$, which are indicators of society's reaction to emerging information in the media.

Let us construct the control function $u(t)$ that allows changing the behavior of the integral curve $N(t)$ so that $N(u(t), t) \rightarrow 0$ for $t \rightarrow +\infty$.

Let us assume that by the time $t = 3$, all the parameters of the system (2) with the values (12) have been determined.

The parameter set (12) does not satisfy the conditions (4). As $\rho = \rho_0 = 5$, we can determine, for example, $u_{\max} = 0,2418$ from which $\rho_{\max} = \rho_0(1 + u_{\max}) = 5(1 + 0,2418) = 6,209$. This means an increase of the average speed of news appearance from one information body by almost 25%.

At the value of the parameter $\rho = \rho_{\max}$ the conditions (4) are fulfilled, and the integral curve $N(t)$ corresponding to this value can be defined as "sample" integral curve.

The graph of this curve is presented in Fig. 4.

Now, let $\Delta t = 1$, $M = 30$ in (7) (this corresponds to the segment of observation of an information event in [18]), and $k = 4$ in (9). The integration results show that before the control begins the values of the integral curves $N(t)$ at $\rho = \rho_0 = 5$ (Fig. 3) and the "sample" integral curve $N^*(t)$ at $\rho = \rho_{\max} = 6,209$ (Fig. 4) differ more and more over time (Fig. 5).

The volume of news information corresponding to the «sample» integral curve $N^*(t)$ from Fig. 5 is presented in Table 4.

Having this data, we can apply an algorithm for building adaptive control.

If $k = 4$, then $u_0 = u_1 = u_2 = 0$. To find u_3 , we find the integral curve $N(u_{\max}, t_4)$ of the system (6) on the segment $[t_3; t_4] = [3; 4]$, having previously defined $N(0, t_3) = 1080.38$ as the initial condition. We

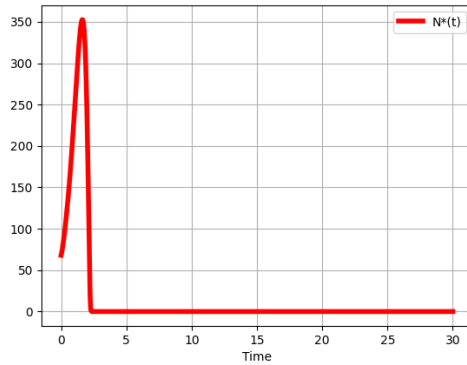


Fig. 4. Integral curve $N^*(t)$ of the system (2) with initial conditions $C(0) = 10, A(0) = 12, N(0) = 68$ and parameter values $\beta = 1,9; \gamma = 0,1; \alpha = 0,09; C_* = 10; \mu = 0,3; \rho = 6,209; \eta = 2,54; \lambda = 1/3$

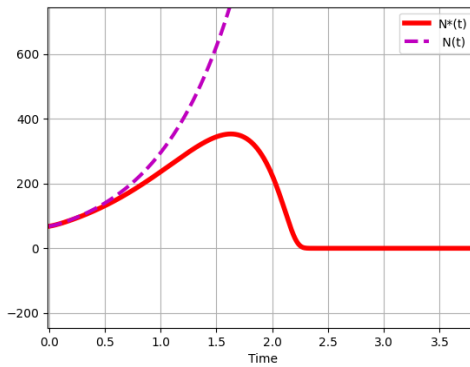


Fig. 5. Integral curves $N(t)$ and $N^*(t)$ before control at time $t_1 = 3$

have $N(u_{\max}, t_4) = 233.85 > N_4^* \approx 0$, so we fix $u_3 = u_{\max}$ on $[t_3; t_4] = [3; 4]$. Next, to find u_4 , we find the integral curve of the system (6) on the segment $[t_4; t_5] = [4; 5]$, taking $= 233.85$ as the initial condition. We have $N(u_{\max}, t_5) = 0 \geq N_5^* = 0$, so we fix $u_4 = u_{\max}$ on $[t_4; t_5] = [4; 5]$. Etc.

Table 4

Number of negative messages $N^*(t)$

t	0	1	2	3	4	5	6	9	12	15	18	...	30
$N^*(t)$	68	235.135	228.409	2E-10	2E-10	0	0	0	0	0	0	0	0

Thus, the control function $u(t)$ (Fig. 6) and its corresponding integral curve $N(u(t), t)$ which gradually approaches the «sample» curve $N^*(t)$ over time (Fig. 7) were obtained through adaptive control.

Table 5 shows the values of $|N(u(t), t) - N^*(t)|$ at points on the grid (7). This corresponds to the satisfaction of the adaptive control criterion (9) for the system (6).

Conclusion

This article presents an algorithm for constructing adaptive control of a system of differential equations, presented as a mathematical model of information confrontation. The feature of this model is that

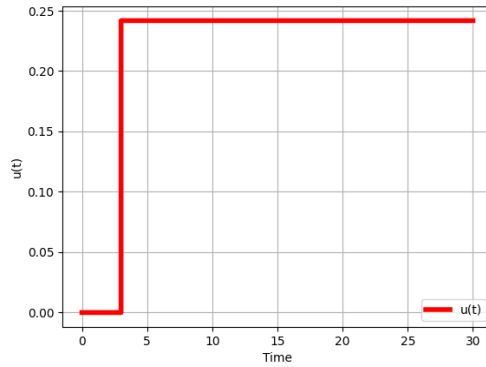


Fig. 6. Control function $u(t)$ during adaptive control from time $t_1 = 3$

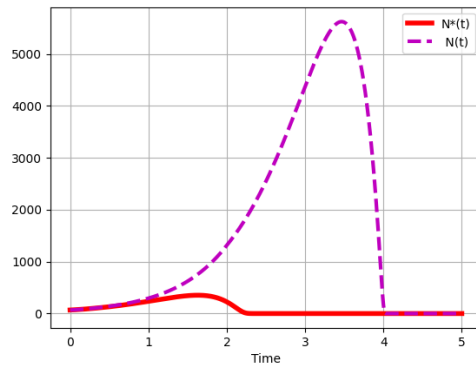


Fig. 7. Integral curves $N(u(t), t)$ and $N^*(t)$ after the start of the control

the subject of modeling is the quantity of information with competing orientations, in contrast to the generally accepted approach that defines the quantity of individuals holding opposing views on some information issue.

Table 5

Values of $|N(u(t), t) - N^*(t)|$ for checking the adaptive control criterion

t	0	1	2	3	4	5	6	9	12	15	18	...	30
$ N(u(t), t) - N^*(t) $	0	59.149	1080.38	4359.1	233.85	0	0	0	0	0	0	0	0

The modern level of technical equipment, such as media monitoring systems and Text Mining, provides the ability to estimate continuously the quality and speed of information flows in real time. These flows, in one way or another, influence the introduction of new (possibly hostile) ideas into public consciousness.

The proposed new approach to modeling allows, in real time, to firstly identify critical situations that could potentially lead to an uncontrolled scenario in the information space. Secondly, it provides the ability to influence the outcome of the confrontation by managing certain parameters (e.g., content, volume, intensity).

In this article, a situation was simulated using a set of parameters determined by Monte Carlo method, where the media disseminates information that could lead to an unfavorable shift in public opinion for government structures.

In the model, this situation is reflected by an uncontrolled growth of one of the components of the system's trajectory, indicating the complete dominance of an antagonistic concept. This necessitated the construction of the control function, which particularly changes the dynamics of the phase variables of the system.

When solving this problem, the following results were obtained:

- For the initial state, obtained from the electronic media monitoring system, the concept of “sample” system trajectory was defined, which moves from the initial point to an asymptotically stable equilibrium of the system. This is only possible, if certain relations are met for the system parameters.
- In the system's parameter space, a component was identified as most suitable for control, allowing the trajectory to be directed towards the “sample” mode.
- A step-by-step algorithm for constructing adaptive system control was proposed, ensuring minimal deviation of the trajectory from the “sample” path after a finite number of steps.
- The proposed algorithm was implemented for numerical integration of the system using the `solve_ivp` module from the SciPy library in Python language.

Substantively, the situation described in the work led to the conclusion that it is necessary to increase the average intensity of news releases by news agencies. By increasing the intensity to the calculated level, there is a real chance to eliminate the adverse effects of an information attack on society.

Thus, the theoretical feasibility of influencing the confrontation between interested parties in promoting their interests through the media has been obtained and justified.

REFERENCES

1. **Marushchak A.V.** Politiko-sotsialnyy obraz Rossii v amerikanskom mediaprostranstve [Political and social image of Russia in the American media space]. *Journalistic Yearbook*, 2012, no. 1, pp. 93–96. (rus)
2. **Sukhodolov A.P., Kuznetsova I.A., Timofeev S.V.** The analysis of approaches in modelling of mass media. *Theoretical and Practical Issues of Journalism*, 2017, Vol. 6, no. 3, pp. 287–305. DOI: 10.17150/2308-6203.2017.6(3).287-305
3. **Dzhashitov V.E., Pankratov V.M., Rezhnikov A.F., Dzhashitov A.E.** Matematicheskoye modelirovaniye i upravleniye v sistemakh informirovaniya i informatsionnogo obmena v obshchestve [Mathematical modeling and control in systems of information and information exchange in society]. *Control Sciences*, 2009, no. 6, pp. 2–8. (rus)
4. **Leonov G.A.** Dinamicheskiye printsipy prognozirovaniya i upravleniya [Dynamic principles of forecasting and control]. *Control Sciences*, 2008, no. 5, pp. 31–35. (rus)
5. **Vyshkind S.Ya., Devetyarova A.A.** On dynamics of some mathematical models in sociology. *Izvestiya VUZ. Applied Nonlinear Dynamics*, 1994, Vol. 2, no. 2, pp. 17–26.
6. **Gubanov D.A., Novikov D.A., Chkhartishvili A.G.** Sotsialnyye seti: modeli informatsionnogo vliyaniya, upravleniya i protivoborstva [Social networks: models of information influence, management and confrontation]. Moscow: Fizmatlit Publ., 2010. 228 p. (rus)
7. **Mikhailov A.P., Marevtseva N.A.** Models of information warfare. *Mathematical Models and Computer Simulations*, 2012, Vol. 4, pp. 251–259. DOI: 10.1134/S2070048212030076
8. **Mikhailov A.P., Petrov A.P., Proncheva O.G., et al.** A model of information warfare in a society under a periodic destabilizing effect. *Mathematical Models and Computer Simulations*, 2017, Vol. 9, pp. 580–586. DOI: 10.1134/S2070048217050106

9. **Mikhailov A.P., Petrov A.P., Proncheva O.G.** A Model of Information Warfare in a Society with a Piecewise Constant Function of the Destabilizing Impact. *Mathematical Models and Computer Simulations*, 2019, Vol. 11, pp. 190–197. DOI: 10.1134/S2070048219020108
10. **Mikhailov A.P., Petrov A.P., Marevtseva N.A., et al.** Development of a model of information dissemination in society. *Mathematical Models and Computer Simulations*, 2014, Vol. 6, pp. 535–541. DOI: 10.1134/S2070048214050093
11. **Doktorov B.Z.** Ot solomennykh oprosov k postgellapovskim oprosnym metodam [From straw polls to post-Gallup polling methods]. Moscow: Raduga Publ., 2013. 72 p. (rus)
12. **Odintsov A.V.** Sociology of public opinion and the Big Data challenge. *Monitoring of Public Opinion: Economic and Social Changes*, 2017, № 3, P. 30–43. DOI: 10.14515/monitoring.2017.3.04
13. **Timofeev S.V., Sukhodolov A.P.** A model of new information dissemination in the society, St. Petersburg Polytechnical State University Journal. *Physics and Mathematics*. 12 (4) (2019) 119–134. DOI: 10.18721/JPM.12412
14. **Timofeev S.V., Baenkhaeva A.V.** Mathematical modeling of information confrontation, St. Petersburg Polytechnical State University Journal. *Physics and Mathematics*. 14 (1) (2021) 164–176. DOI: 10.18721/JPM.14113
15. **Timofeev S.V., Baenkhaeva A.V.** Modeling of information confrontation: Research directions and mathematical tools. *Computing, Telecommunications and Control*, 2022, Vol. 15, No. 2, Pp. 63–75. DOI: 10.18721/JCSTCS.15205
16. **Samarskii A.A., Mikhailov A.P.** Matematicheskoe modelirovanie: Idei. Metody. Primery [Mathematical Modeling: Ideas. Methods. Examples]. M.: Fizmatlit, 2001. 320 p. (rus)
17. **Trusov P.V.** Vvedenie v matematicheskoe modelirovanie [Introduction to mathematical modeling]. Moscow: Logos Publ., 2005. 440 p. (rus)
18. **Timofeev S.V., Baenkhaeva A.V., Abdullin V.R.** Verification of the Adequacy of the Dynamic Model of Information Confrontation Based on Electronic Media Monitoring Data on the Coverage of the Events of January 2022 in Kazakhstan. *System Analysis & Mathematical Modeling*, 2023, Vol. 5, no. 2, pp. 153–171. DOI: 10.17150/2713-1734.2023.5(2).153-171
19. **Arrowsmith D.K., Place C.M.** Ordinary Differential Equations: A Qualitative Approach with Applications. London, NY: Chapman & Hall, 1982. 252 p.
20. **Fomin V.N., Fradkov A.L., Yakubovich V.A.** Adaptivnoe upravlenie dinamicheskimi ob"ektami [Adaptive Control of Dynamic Objects]. Moscow: Nauka, 1981. 447 p. (rus)
21. SciPy API – SciPy v1.14.0 Manual, Available: <https://docs.scipy.org/doc/scipy/reference/> (Accessed 01.09.2023)
22. solve_ivp – SciPy v1.14.0 Manual, Available: https://docs.scipy.org/doc/scipy/reference/generated/scipy.integrate.solve_ivp.html (Accessed 01.09.2023)
23. **Kong Q., Siau T., Bayen A.M.** Python Programming and Numerical Methods: A Guide for Engineers and Scientists. Amsterdam: Elsevier Inc., 2020. 456 p. DOI: 10.1016/C2018-0-04165-1

INFORMATION ABOUT AUTHORS / СВЕДЕНИЯ ОБ АВТОРАХ

Timofeev Sergey V.
Тимофеев Сергей Викторович
 E-mail: timofeevsv12@gmail.com

Baenkhaeva Ayuna V.
Баенхаева Аюна Валерьевна
 E-mail: ayunab2000@mail.ru

Submitted: 22.01.2024; Approved: 24.06.2024; Accepted: 15.07.2024.

Поступила: 22.01.2024; Одобрена: 24.06.2024; Принята: 15.07.2024.

Research article

DOI: <https://doi.org/10.18721/JCSTCS.17205>

UDC 681.513.1



APPROACHES AND PRINCIPLES FOR ADVANCED CONTROL OF A MULTI-FLOW TUBE FURNACE

E.S. Gebel  

Peter the Great St. Petersburg Polytechnic University,
St. Petersburg, Russian Federation

 gebel_es@spbstu.ru

Abstract. To improve the efficiency of multi-flow tube furnaces, a multi-parameter advanced cohesive control system is proposed. Stabilization of the main technological parameter, i.e. the resulting temperature of the output material flow, is carried out by supervisory control of flow rates on the inlet coils, taking into account the existing limitation on the loading of the apparatus, while meeting the requirement of a uniform temperature profile. To create an optimal combustion mode, an additional circuit for regulating the discharge in the radiant chamber of the furnace on the line of atmospheric air supply to the burner registers according to the residual oxygen content in the flue gases is introduced. In the developed simulation model of the control system the possibility of shockless transition between the basic, as in production, and advanced variants of the control system is realized. Transfer functions of the multilink control object, as well as the tuning parameters of the regulators on individual channels are obtained by the built-in tools of Matlab Simulink. Computational experiments on the model showed high speed and control accuracy.

Keywords: multi-flow furnace, cohesive control system, simulation model, temperature profile, efficiency factor

Citation: Gebel E.S. Approaches and principles for advanced control of multi-flow tube furnace. Computing, Telecommunications and Control, 2024, Vol. 17, No. 2, Pp. 52–61. DOI: 10.18721/JCSTCS.17205

Научная статья

DOI: <https://doi.org/10.18721/JCSTCS.17205>

УДК 681.513.1



ПОДХОДЫ И ПРИНЦИПЫ УСОВЕРШЕНСТВОВАННОГО УПРАВЛЕНИЯ МНОГОПОТОЧНОЙ ТРУБЧАТОЙ ПЕЧЬЮ

Е.С. Гебель  Санкт-Петербургский политехнический университет Петра Великого,
Санкт-Петербург, Российская Федерация gebel_es@spbstu.ru

Аннотация. Для повышения эффективности работы многопоточных трубчатых печей предложена многопараметрическая усовершенствованная система связанного управления. Стабилизация основного технологического параметра – результирующей температуры выходного материального потока, осуществляется путем супервизорного управления расходами на входных змеевиках с учетом имеющегося ограничения на загрузку аппарата, при выполнении требования равномерного температурного профиля. Для создания оптимального режима горения введен дополнительный контур регулирования разряжения в радиантной камере печи на линии подачи атмосферного воздуха к регистрам горелок по содержанию остаточного кислорода в дымовых газах. В разработанной имитационной модели системы управления реализована возможность безударного перехода между базовым, как на производстве, и усовершенствованным вариантами. Передаточные функции многосвязного объекта управления, а также параметры настройки регуляторов по отдельным каналам получены встроенными инструментами Matlab Simulink. Вычислительные эксперименты на модели показали высокое быстродействие и точность регулирования.

Ключевые слова: многопоточная печь, система связанного управления, имитационная модель, температурный профиль, КПД

Для цитирования: Gebel E.S. Approaches and principles for advanced control of multi-flow tube furnace // Computing, Telecommunications and Control. 2024. Т. 17, № 2. С. 52–61. DOI: 10.18721/JCSTCS.17205

Introduction

Tube furnaces are the main apparatuses providing thermal regime of technological processes in oil refining and petrochemical industries. Multi-flow tube furnaces are a component of various plants of high-temperature thermos-technological and chemical processes, such as devices for distillation of oil or fuel oil, pyrolysis, catalytic cracking, reforming, hydrotreating, realize heating, evaporation and superheating of liquid and gaseous media [1, 2]. Increasing the efficiency of such apparatuses allows to minimize its consumption, hence, reduces the amount of harmful carbon dioxide emissions into the atmosphere [3, 4]. Implementation of high-tech solutions of industrial automation at the considered apparatus is aimed at optimizing fuel consumption for processing a ton of oil.

A typical control scheme for thermal objects involves regulating the common flow temperature at the furnace output by varying the fuel gas pressure. In production, under the given limitation of the device load, the operator manually sets the same settings for the flow controllers on each coil. As a result, the temperature profile of the output streams is non-uniform, which leads to a decrease in efficiency [2, 4]. The proposed scheme of advanced process control of temperature deviation at the output of the tube furnace coils by the flow rate of the input streams, taking into account the limitation of the apparatus loading will allow the operator to quickly change the value of the flow rate settings and provide a uniform temperature profile (Fig. 1, *a*).

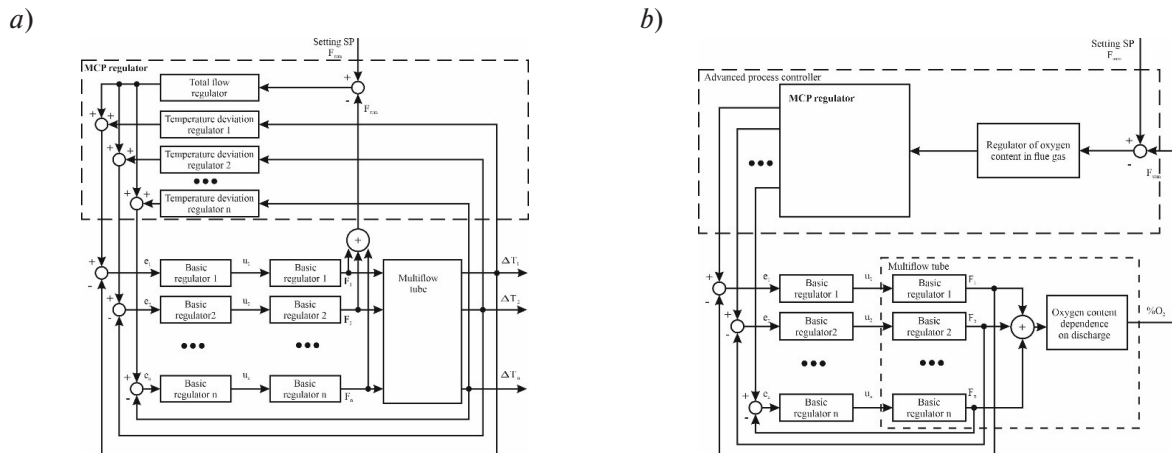


Fig. 1. General structure of control schemes:

a) furnace temperature profile, b) residual oxygen concentration in flue gas

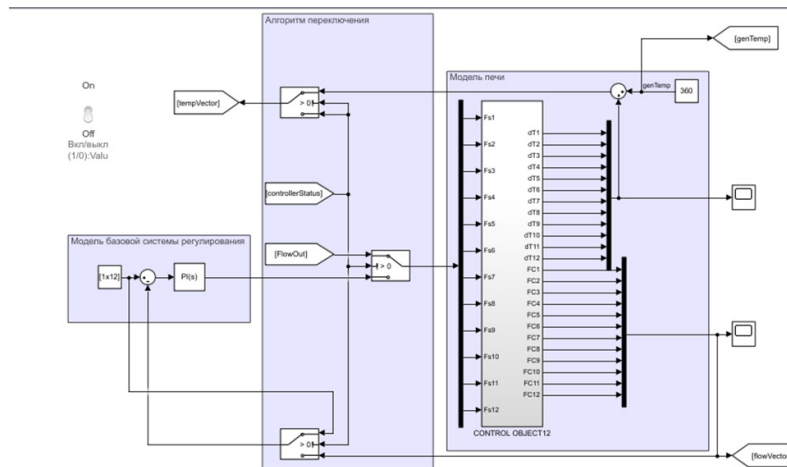


Fig. 2. Simulation model of the control object

Another way to increase the efficiency of the plant is the use of oxygen correction in the flue gases (Fig. 1, b). At furnace load of 50% and higher, the oxygen concentration in the flue gases should be from 3% to 4%, which corresponds to the required amount of excess air in the burner for complete combustion of fuel [2, 5]. It has been noted that excess air in flue gases is observed in almost all furnaces operating for more than 15–20 years [1, 2, 6, 7]. This may be caused by improper operation of the burner register or non-tightness of the construction. The maximum efficiency of apparatus is achieved at such excess air, when losses caused by incomplete combustion and heat carried away by flue gases are minimized [2, 6]. Stabilization of oxygen in the flue gases (Fig. 1b) will provide optimal rarefaction in the radiant chamber of the tube furnace, and, consequently, will increase the efficiency.

Thus, it seems relevant to develop approaches and principles for advanced control of a multi-flow tube furnace to improve the efficiency of the plant.

Simulation model of the control object

Elements of the simulation model of the technological object (Fig. 2) are united into blocks “Basic control model”, “Switching algorithm” and “Furnace model” by functional feature.

The subsystem “Algorithm of switching” (Fig. 2) contains three switches to set the operation modes of the control system. The high level of the ControllerStatus logic signal satisfies the choice of the advanced variant of the control system. The FlowOut load is used either as a limitation or to calculate vector elements in the “Basic control model” block representing the settings of the flow rate regulators on the furnace input flows.

The subsystem “Furnace Model” describes the dynamics of the channels “temperature deviation – input flow rate”. The mathematical model of the technological apparatus depends on the research objectives and complexity of the object under consideration and is formed either on the laws of physics, chemistry, heat engineering and other fundamental sciences [8, 9], or on statistical methods or machine learning methods [10–13]. “Lifetime” of the simulation model is limited due to the instability of physical and chemical parameters of input streams and random impact of the environment, which leads to continuous changes in technical characteristics, as a consequence, the parameters of the object [15, 16]. Taking into account the connectivity of control channels and variation of parameters of the studied technological object, the mathematical model represents a matrix in the following form:

$$W(s) = \begin{pmatrix} W_{11}(s) & W_{12}(s) & \dots & W_{1n}(s) \\ W_{21}(s) & W_{22}(s) & \dots & W_{2n}(s) \\ \dots & \dots & \dots & \dots \\ W_{n1}(s) & W_{n2}(s) & \dots & W_{nn}(s) \end{pmatrix}. \quad (1)$$

Each element in formula (1) describes the effect of the i -th input (flow rate on the i -th flow) on the j -th output (temperature deviations from the set resultant value on the j -th coil) signal. The parameters i and j vary from 1 to n , where n is the number of coils in the design of multi-flow furnace.

Further in the work the object is considered as linear, thus, the expression for the j -th output flow is:

$$W_1(s) = W_{11}(s) + W_{21}(s) + \dots + W_{n1}(s). \quad (2)$$

The structure of transfer functions $W_{ij}(s)$ in the matrix (1) corresponds to the dynamic link of the second order with delay. This is valid for the majority of technological objects [17–19]:

$$W_{ij}(s) = \frac{K_{ij}}{T_{2ij}s^2 + T_{1ij}s + 1} e^{-\tau_{ij}s}, \quad (3)$$

Parameter K_{ij} is a transmission coefficient at the ij -th control channel. Time constants denotes as T_{1ij} , T_{2ij} , and lag time is as τ_{ij} .

Identification of the parameters K_{ij} , T_{1ij} , T_{2ij} and τ_{ij} in (3) from historical data of the technological process from the plant is performed by various computational methods [12, 14, 17, 18] using the built-in Matlab Simulink tools. It was found that the highest values of the transmission coefficient of about 0.8 have the following control channels: $W_{11}(s)$, $W_{22}(s)$, ... $W_{nn}(s)$; for the rest $W_{ij}(s)$ ($i \neq j$) this parameter varies within ± 0.1 [19]. The variation of parameters K_{ij} , T_{1ij} and T_{2ij} , caused by the action of various internal and external factors, was taken into account by introducing additional elements $K_r \cdot r$ and $T_r \cdot r$ in the transfer function. Parameter r sets the permissible limits of variation. This is a random number with a normal distribution law, varying within $0 \div 1$. Thus, in general, the transfer functions for the individual control channels “flow rate – flow temperature deviation” have the following form:

$$W_{ij}(s) = \frac{(K_{ij} + K_r r)}{(T_{2ij} + T_r r)s^2 + (T_{1ij} + T_r r)s + 1} e^{-\tau_{ij}s}. \quad (4)$$

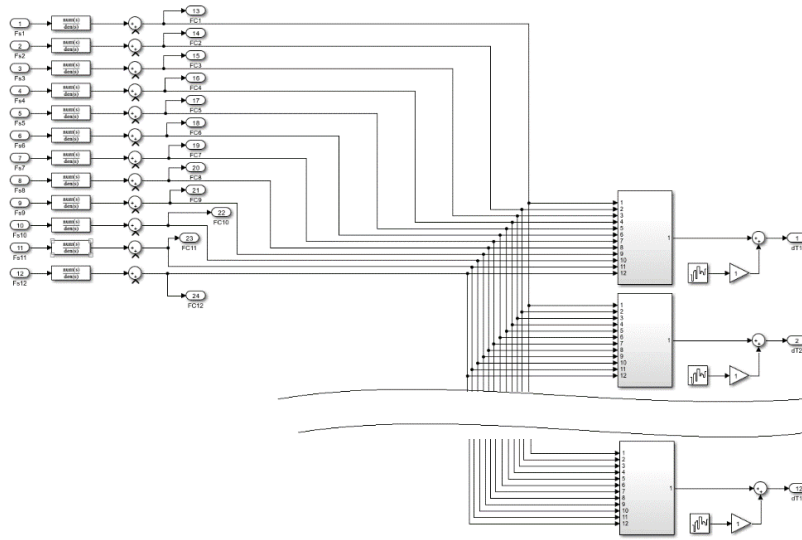


Fig. 3. Structure of subsystem “Furnace model”

Coefficients K_r , T_r calculated based on the accumulated experience of safe and accident-free operation of the plant.

The subsystem “Furnace Model” (Fig. 3) contains groups of elements simulating the dynamics of the flow sensors (block 1), additional outputs to monitor the fulfilment the limitation of the total unit load (block 2), and individual control channels (block 3) in accordance with logic and structure of the model (2), (4).

Advanced process control of a multi-flow tube furnace

The structure of the simulation model of the advanced process control of a multi-flow atmospheric tube furnace develops based on the subsystem “Simulation model of the control object” (Fig. 2) and is shown in Fig. 4.

The resulting temperature of the total flow sets in accordance with the requirements of the technology and regulates in proportional to the ratio of fuel consumption and atmospheric air [1–3, 10]. Based on the temperature data in the total flow at the output of the GenTemp furnace and the temperature vector on individual coils TempVector obtained from the subsystem in Fig. 2, the average temperature deviation dTmean is automatically corrected (Fig. 4). Classical control laws [21–23] were used, which, in comparison with the intelligent control methods, have higher performance [9, 10, 15, 20]. Thus, a PI controller applies in the external loop in the TempBlock subsystem (Fig. 4), the values of the tuning coefficients PI_temp_P and PI_temp_I, as well as the width of the insensitivity zone dzTemp, were calculated using the built-in Matlab Simulink tools. Additionally, protection against the integral oversaturation was implemented in the TempAggrIntegrator1 block of the advanced control system.

The connected flow control loop on the inputs is represented in Fig. 4 by FlowBlock, the regulator is realized as a PI controller with settings: PI_Flow_P, PI_Flow_I and dzFlow. The vector of logical variables FlowModeVector reflects the current structure of the tube furnace (number of operating threads). Zero values of elements correspond to the flow shutdown, for example, for scheduled maintenance. The input signal FlowErrorVector contains the settings either calculated in the external loop TempBlock or set manually by the matrix in the “Basic control model” block (Fig. 2).

Setup of regulators in the internal FlowBlock and external TempBlock1 loops is performed using the built-in Matlab Simulink tools according to the criterion of maximum robustness of the system. There is

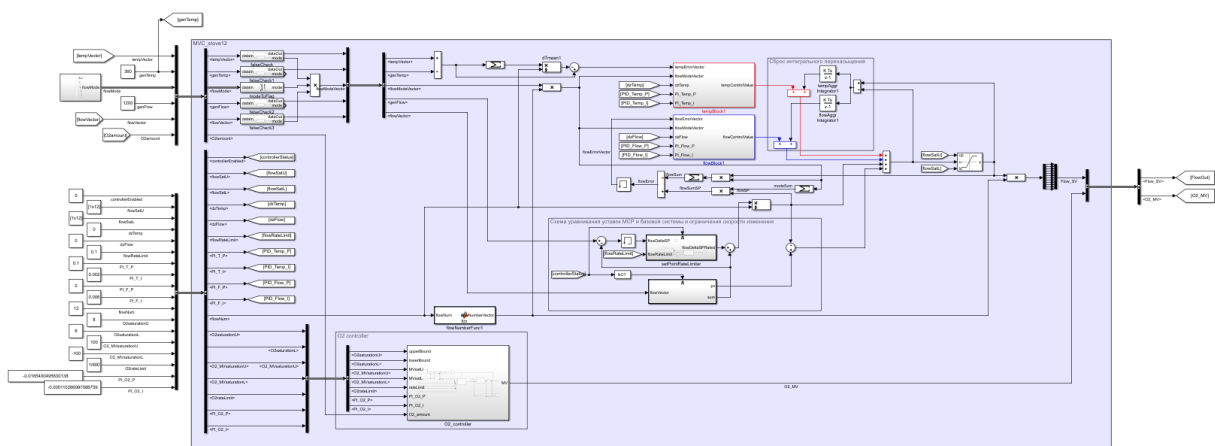


Fig. 4. Simulation model of the advanced process control of the multi-flow atmospheric tube furnace

a possibility to exclude some flows Block “Object Structure” (Fig. 4), which is in demand, for example, during maintenance of automation equipment on a particular coil.

In addition, shockless switching between variants of the control system (Fig. 4) of a multi-flow tube furnace implements due to equalizing the settings. Low level of the ControllerStatus logic signal returns the system to the basic variant of control. Then, the current value of the total unit load, calculated in the subsystem “Furnace Model” (Fig. 3, block 2) of the advanced system, is memorized. After that, the settings of the flow controllers for each flow are calculated in the block Shockless_Switching.

The setPointRateLimiter subsystem (Fig. 4) sets a limit on the rate of change of settings by the built-in Matlab function. It generates an output signal equals to the difference between the current value of flow rates and settings for individual flows in the advanced control system. The memory element eliminates errors during the model simulation run. In addition, the absolute value (Saturation block) on the upper or lower limits (flowSatU or flowSatL) of the settings is limited. Reaching these values activates the reset aggravation function “Reset integral oversaturation” (Fig. 4).

The internal structure of the “O₂ controller” subsystem is shown in Fig. 5. The concentration of residual oxygen in the flue gases (O₂ amount signal) has a long lag time. Therefore, a “gating” signal is supplied to the “O₂ Block” to stop the control process, when the output parameter reaches the UpperBound or LowerBound values.

The maximum permissible values of the discharge in the radiant chamber of the tube furnace MVsatU and MVsatL are the parameters of “O₂ Block” regulator. This feature is critical for the considered apparatus. Both the absolute value of the setting MeanErr and the rate of its increase RateLimit forms in the “O₂ Rate” block. The control actions on the gate valves in the atmospheric air supply line to the burner registers are discrete signals.

Approbation of the advanced process control

The effectiveness of the proposed approaches and principles of the advanced process control of the multi-flow tube furnace was evaluated by means of model tests, the results of which are presented in Fig. 6. It was required to estimate the stability of the transient process for the basic and proposed control systems, and to calculate the control quality indicators, in particular, performance and accuracy.

Transient graphs (Fig. 6, a), obtained when switching the control system from the basic to the advanced scheme at 2600 seconds, demonstrates the narrowing of the range of temperature variation of individual streams and the establishment of the set value of the resulting temperature after 1400 seconds. The flow rates of the input streams dynamically change, taking values within (89÷91) m³/h, which is

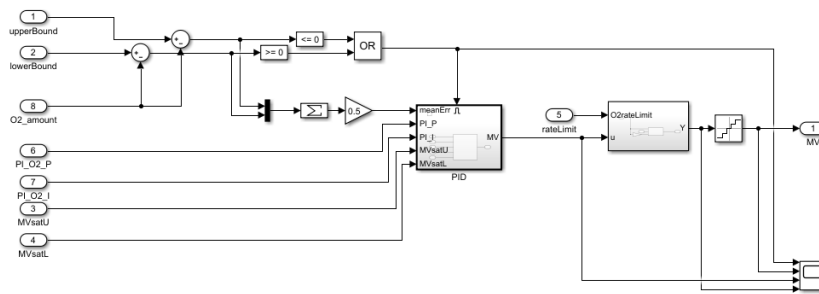


Fig. 5. Structure of “O2 controller” subsystem

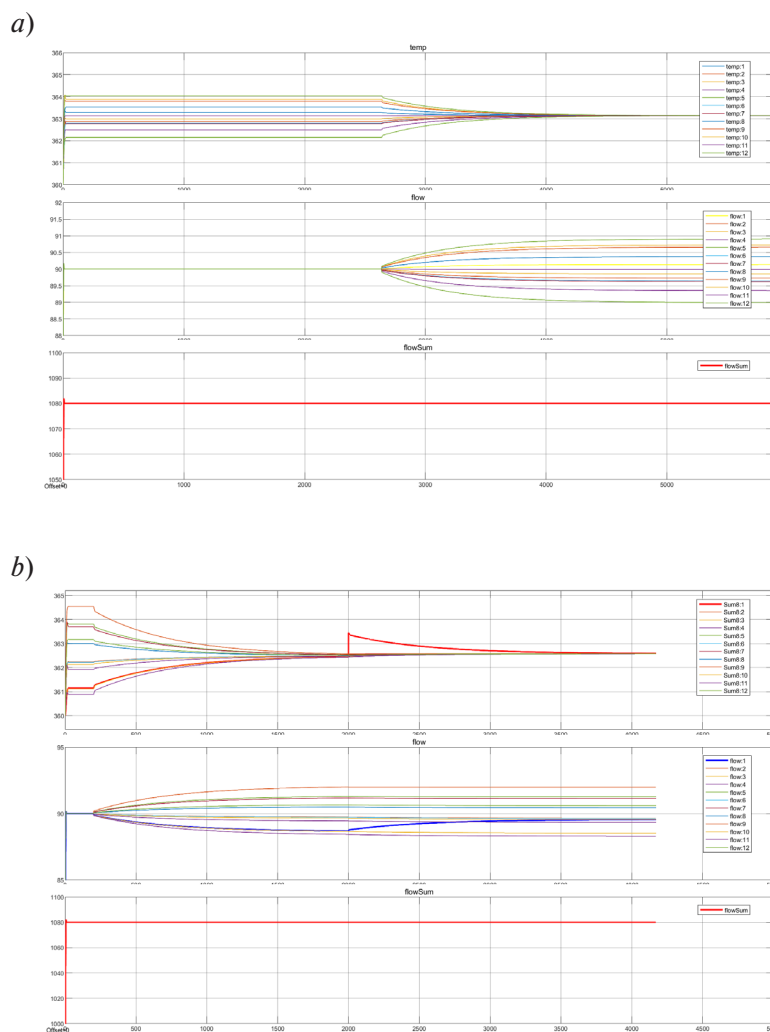


Fig. 6. Results of model tests of the control system:

a) when switching between variants of control systems, b) when perturbation is applied

allowed by the technological regulations. The furnace load volume for both control schemes remains constant at 1080 m³/h.

The output signal of the model, when a temperature perturbation (1° increase compared to the calculated one) arrives at the first coil at 2000 seconds, quickly reaches the set steady-state value, and the

static error equals zero. The temperature deviation is compensated after 700 seconds (Fig. 6, *b*). Numerical experiments performed on the simulation model of the system of advanced process control of a multi-flow tube furnace allows to conclude that the performance results are satisfactory in terms of control quality.

Conclusion

Improved efficiency of the multi-flow atmospheric furnace of the oil refining apparatus is achieved by implementing the proposed approaches and principles of advanced process control. The uniform temperature profile of the output flows indicates the optimality of combustion conditions in the radiant chamber.

The mathematical model of control object dynamics developed taking into account connectivity and random variation of technical parameters of control channels to improve its accuracy and “lifetime”. Another advantage of the proposed approach is the scalability of the simulation model, which allows to manually exclude part of the flows from the analysis. The change in the control object structure is compensated by the random component in the transfer functions of each channel. This principle is especially demanded, when the object is operated in continuous production. The system of advanced process control provides compensation of integral saturation of regulators, robustness to small fluctuations of technical parameters of the control object, and realizes the “gating” mode on the channel of residual oxygen in flue gases.

Thus, the implementation of the proposed approaches and principles of advanced process control of the multi-flow tube furnace of oil refining apparatus will increase the coefficient of utilization of the heat of combustion of fuel, decrease the volume of fuel consumed, as a consequence, reduce harmful carbon dioxide emissions into the atmosphere.

REFERENCES

1. **Zhidkov A.B., Gerasimov D.P., Denisov D.E. i dr.** Trubchatye nagrevatel'nye pechi neftepererabotki i neftekhimii [Tube heating furnaces for oil refining and petrochemicals]. SPb.: ArtProekt, 2015. 102 p.
2. **Jenkins B., Mullinger P.** Industrial and Process Furnaces. Principles, Design and Operation. Elsevier Ltd, 2023. 661 p. DOI: 10.1016/C2020-0-04546-9
3. **Lipin A.A., Lipin A.G.** Raschet trubchatykh pechei [Calculation of tube furnaces]. Ivanovo: Izd-vo Ivanov. gos. khim.-tehnolog. un-ta, 2019. 80 s.
4. **Safarova A., Melikov E., Magerramova T.** Control of a Tube Furnace in Conditions of Risk and Increased Explosion Hazard. Reliability: Theory & Applications, Special Issue. 2022, Vol. 17, no. 4 (70), pp. 516–521.
5. **Pavlechko V.N., Frantskevich V.S.** Influence of oxygen concentration on the process of combustion gas fuel // Trudy BGTU. Ser. 2: Khimicheskie tekhnologii, biotekhnologii, geoekologii [Proceedings of Shukhov Belgorod State Technological University. Series 2: Chemical technologies, biotechnology, geoecology]. 2018, Vol. 211, no. 2, pp. 100–105.
6. **Riabchikov M.IU., Riabchikova E.S., Obukhova T.G.** Sistema optimizatsii upravleniia protsessom szhiganiia topliva na osnove informatsii o sodержanii kisloroda v otkhodiashchikh dymovykh gazakh [System of optimization of fuel combustion process control based on information on oxygen content in waste flue gases]. Elektrotekhnicheskie sistemy i kompleksy [Electrical systems and complexes]. 2012, Vol. 20, pp. 316–320.
7. **Torgashov A.Iu.** Modelirovanie dinamiki i issledovanie optimal'nogo funktsionirovaniia teploobmenno-go tekhnologicheskogo protsessa [Modeling of dynamics and study of optimal functioning of heat-exchange technological process]. Informatika i sistemy upravleniia [Informatics and control systems]. 2011, Vol. 28, no. 2, pp. 86–93.

8. **Sobolev O.S.** Razvitie funktsii kontrolya i upravleniya v ASU nepreryvnymi tekhnologicheskimi protsessami [Development of monitoring and control functions in the automated control system of continuous technological processes]. M.: INFORMPribor, 1990. 60 p.

9. **Faruntsev S.D., Gebel E.S.** Advanced process control system oil-gas separator by the temperature channel. Journal of Physics: Conference Series. 2019, Vol. 1210, Article no. 012042. DOI: 10.1088/1742-6596/1210/1/012042

10. **Denisova L.A., Alekseitsev D.M.** Developing a supervisory control system based on fuzzy logical inference. Avtomatizatsiya v promyshlennosti [Automation in industry]. 2019, Vol. 1, pp. 46–52. DOI: 10.25728/avtprom.2019.01.07

11. **Kutsyi N.N., Lukyanov N.D.** Control system synthesis by a multivariable object using the genetic algorithm (on the example of the once-through boiler). Scientific Bulletin of NSTU. 2014, Vol. 55, no. 2, pp. 36–42.

12. **Nehal N., Lounis Z., Bouhadiba B., Lounis Z.** Modelling of heating furnace fire scenarios using fault tree analysis, a Bayesian network, and a thermal transfer method for system reliability analysis. Journal of Loss Prevention in the Process Industries. 2023, Vol. 83, Article no. 104995. DOI: 10.1016/j.jlp.2023.104995

13. **Dozortsev V.M.** Digital twins in industry: genesis, structure, terminology, technologies, platforms, outlook. Part 2 – Key digital twin technologies. Physical object modeling types. Avtomatizatsiya v promyshlennosti [Automation in industry]. 2020, Vol. 11, pp. 3–10. DOI: 10.25728/avtprom.2020.11.01

14. **Zhu Y., Yang C., Chen X., Zhou J., Zhao J.** Identification-based real-time optimization and its application to power plants. Control Engineering Practice. 2022, Vol. 123, Article no. 105160. DOI: 10.1016/j.conengprac.2022.105160

15. **Chenliang W., Yan L.** Adaptive dynamic surface control for linear multivariable systems. Automatica. 2010, Vol. 46, no. 10, pp. 1703–1711. DOI: 10.1016/j.automatica.2010.06.020

16. **Zhiteckii L.S., Azarskov V.N., Solovchuk K.Yu., Sushchenko O.A.** Discrete-time robust steady-state control of nonlinear multivariable systems: a unified approach. IFAC Proceedings Volumes. 2014, Vol. 47, no. 3, pp. 8140–8145. DOI: 10.3182/20140824-6-ZA-1003.01985

17. **Sun Y.-N., Zhuang Z.-L., Xu H.-W., Qin W., Feng M.-J.** Data-driven modeling and analysis based on complex network for multimode recognition of industrial processes. Journal of Manufacturing Systems. 2022, Vol. 62, pp. 915–924. DOI: 10.1016/j.jmsy.2021.04.001

18. **Chaves C.R., Rodrigo J.C.G., Gartia C.** Identification of the dynamic model of a petrochemical furnace of 50MW for implementation of MPC control. IFAC-PapersOnline. 2019, Vol. 52, no. 1, pp. 317–322. DOI: 10.1016/j.ifacol.2019.06.081

19. **Teslov K.S.** Razrabotka demonstratsionnogo maketa mnogovsvyaznoi sistemy regulirovaniya mnogopotочноi pechi [Development of a demonstration layout of a multi-linked control system for a multi-flow furnace]. Avtomatizatsiya, mekhatronika, informatsionnye tekhnologii [Automation, mechatronics, information technologies]. 2020, pp. 23–29.

20. **Abilov A.G., Zeybek Z., Tuzunalp O., Telatar Z.** Fuzzy temperature control of industrial refineries furnaces through combined feedforward/feedback multivariable cascade systems. Chemical Engineering and Processing. 2002, Vol. 41, no. 1, pp. 87–98. DOI: 10.1016/S0255-2701(01)00119-2

21. **Feliu-Batlle V., Rivas-Perez R.** Control of the temperature in a petroleum refinery heating furnace based on a robust modified Smith predictor. ISA Transactions. 2021, Vol. 112, pp. 251–270. DOI: 10.1016/j.isatra.2020.12.006

22. **Luan X., Chen Q., Liu F.** Centralized PI control for high dimensional multivariable systems based on equivalent transfer function. ISA transactions. 2014, Vol. 53, no. 5, pp. 1554–1561. DOI: 10.1016/j.isatra.2014.05.016

23. **Ram V.D., Chidambaram M.** Simple method of designing centralized PI controllers for multivariable systems based on SSGM. ISA transactions. 2015. Vol. 56, pp. 252–260. DOI: 10.1016/j.isatra.2014.11.019

INFORMATION ABOUT AUTHOR / СВЕДЕНИЯ ОБ АВТОРЕ

Gebel Elena S.

Гебель Елена Сергеевна

E-mail: gebel_es@spbstu.ru

ORCID: <https://orcid.org/0000-0003-1811-8755>

Submitted: 13.02.2024; Approved: 16.07.2024; Accepted: 30.07.2024.

Поступила: 13.02.2024; Одобрена: 16.07.2024; Принята: 30.07.2024.

Intelligent Systems and Technologies

Интеллектуальные системы и технологии

Research article

DOI: <https://doi.org/10.18721/JCSTCS.17206>

UDC 004.932.72



COMPARISON AND SELECTION OF RADIOMIC AND DEEP CONVOLUTIONAL FEATURES FOR IMPROVING THE ACCURACY OF CT-IMAGE TEXTURE CLASSIFICATION

F. Shariaty  , *V.A. Pavlov* , *M.U. Surakov*

Peter the Great St. Petersburg Polytechnic University,
St. Petersburg, Russian Federation

 shariaty3@gmail.com

Abstract. The article explores the problem of comparing and selecting radiomic and deep convolutional features extracted from CT images to enhance the accuracy of texture classification in CT diagnostics. By using the mRMR method, the study assesses the significance of these features in predicting genetic mutations in patients with lung cancer, highlighting their importance for refining diagnostic procedures. The developed predictive model demonstrates high classification accuracy of 92%, which indicates its high efficiency. Analysis of the results reveals that deep learning features effectively capture complex, high-level abstract textures that indicate the presence of pathologies. At the same time, radiomic features provide key information about the phenotypic characteristics of tumors, such as shape, texture, and intensity. This comprehensive approach not only improves the accuracy of non-invasive diagnostics, but also contributes significantly to personalized medicine by facilitating the development of more precise treatment strategies based on genetic profiles.

Keywords: radiomics, deep convolutional features, computed tomography, machine learning, feature selection

Acknowledgements: The research was supported by the Russian Science Foundation grant No. 24-25-00204 “Integrating genomic analysis and medical imaging to accurately predict and predict cancer characteristics and treatment outcomes in early-stage non-small cell lung cancer”. Available online: <https://rscf.ru/project/24-25-00204/>

Citation: Shariaty F., Pavlov V.A., Surakov M.U. Comparison and selection of radiomic and deep convolutional features for improving the accuracy of CT-image texture classification. *Computing, Telecommunications and Control*, 2024, Vol. 17, No. 2, Pp. 62–70. DOI: 10.18721/JCSTCS.17206

Научная статья

DOI: <https://doi.org/10.18721/JCSTCS.17206>

УДК 004.932.72



СРАВНЕНИЕ И ВЫБОР РАДИОМИЧЕСКИХ И ГЛУБОКИХ СВЕРТОЧНЫХ ПРИЗНАКОВ ДЛЯ ПОВЫШЕНИЯ ТОЧНОСТИ КЛАССИФИКАЦИИ ТЕКСТУР КТ-ИЗОБРАЖЕНИЙ

Ф. Шариати , В.А. Павлов , М.У. Сураков

Санкт-Петербургский политехнический университет Петра Великого,
Санкт-Петербург, Российская Федерация

 shariaty3@gmail.com

Аннотация. В статье подробно рассматривается задача сравнения и выбора радиомических и глубоких сверточных признаков, извлекаемых из КТ-изображений, для повышения точности классификации текстур в рамках КТ-диагностики. Использование метода mRMR позволило оценить значимость этих признаков в контексте прогнозирования наличия генетических мутаций у пациентов с раком легкого, подчеркивая их важность для уточнения диагностических процедур. Разработанная модель показала высокую точность классификации – 92%, что свидетельствует о ее высокой эффективности. Анализ результатов выявил, что признаки, основанные на глубоком обучении, эффективно фиксируют сложные, высокоуровневые абстрактные текстуры, что указывает на наличие патологий. В то же время радиомические признаки обеспечивают ключевую информацию о детальных фенотипических характеристиках опухолей, включая форму, текстуру и интенсивность. Такой комплексный подход не только повышает точность неинвазивной диагностики, но и вносит значимый вклад в персонализированную медицину, способствуя разработке более точных стратегий лечения на основе генетических профилей.

Ключевые слова: радиомика, глубокие сверточные признаки, компьютерная томография, машинное обучение, отбор признаков

Финансирование: Исследование выполнено за счет гранта Российского научного фонда № 24-25-00204 «Интеграция геномного анализа и медицинской визуализации для точного прогнозирования и предсказания характеристик рака и результатов лечения при ранней стадии неклеточного рака легкого», <https://rscf.ru/project/24-25-00204/>

Для цитирования: Shariaty F., Pavlov V.A., Surakov M.U. Comparison and selection of radiomic and deep convolutional features for improving the accuracy of CT-image texture classification // Computing, Telecommunications and Control. 2024. Т. 17, № 2. С. 62–70. DOI: 10.18721/JCSTCS.17206

Introduction

Image processing and analysis now occupy an important place in many areas of science and technology. The ability to accurately analyze and interpret images is particularly critical in medical imaging, where it can directly impact diagnostic capabilities. The development of new feature extraction methods not only contributes to the accuracy of analysis, but also opens new opportunities for early diagnosis and personalized treatment approach [1].

Recent advances in radiomics and deep learning have opened new horizons in extracting and analyzing complex features from medical images. Radiomics involves extracting a large number of features from medical images [2]. On the other hand, deep learning, especially convolutional neural networks (CNN), has shown success in image classification tasks [3, 4].

Radiomic features, although informative, may not cover the full range of available information in the images under study. Deep learning models often act as “black boxes”, providing little information

about features that have a greater impact on decision making in image classification. In addition, the performance of these models can depend significantly on the quality and quantity of training images.

This paper proposes the results of a comparative analysis of radiomic and deep convolutional features on CT images to classify textures indicating the presence or absence of genetic mutations in patients with lung cancer. The aim of this study is to improve the accuracy of CT image texture classification by jointly using the most effective radiomic and deep convolutional features.

Materials and methods

Data collection and pre-processing

This study used dataset [5] which contains diagnostic and prognostic information such as: CT images, semantic annotations, gene mutation status information.

Deep learning features

Deep convolutional feature extraction was performed using the pre-trained ResNet18 [2], which was chosen because of its relatively simple structure compared to deeper models, facilitating faster training and image processing while still being able to extract complex features. The model was adapted for the task by removing the last classification layer, allowing it to function as a feature generator that generates a deep convolutional feature vector from the last convolutional layer immediately preceding the classification layer. The vector consists of 512 floating point numbers («Deep feature 1», ..., «Deep feature 512») and encompasses high-level representations of CT images learned by the model from a large number of images. These representations are assumed to include textures related to tumor morphology and possibly indirect markers of genetic mutations. The extracted features were used as part of an integrated feature set, contributing model-derived knowledge to the classification process.

Radiomic features extraction

Radiomic features play a key role in describing pulmonary nodule texture features on CT images. The first extraction step begins with segmentation of pulmonary nodules, using either manual annotation by expert radiologists or automated segmentation algorithms. This segmentation is then used for quantitative analysis, where radiomic features are systematically extracted and classified into three main groups [6–8]:

- **First-order statistics:**

- *Mean intensity*. Mean intensity represents the average of the pixels within a nodule image and is a basic measure of its overall brightness. Mathematically it is expressed as follows:

$$\mu = \frac{1}{N} \sum_{i=1}^N x_i,$$

where x_i is intensity value of the i -th pixel, a N is the total number of pixels in the nodule. Mean intensity indicates average nodule density.

- *Standard deviation*. Standard deviation quantifies the variation of intensity values around the mean value, reflecting heterogeneity within the nodule. A larger standard deviation implies a wider range of intensity values, indicating variability in nodule composition. The standard deviation is calculated by the formula:

$$\sigma = \sqrt{\frac{1}{N-1} \sum_{i=1}^N (x_i - \mu)^2}.$$

This index gives an indication of the texture of the nodule.

- *Skewness*. Skewness measures the asymmetry of the intensity distribution around the mean value. Skewness is defined as:

$$Skewness = \frac{\frac{1}{N} \sum_{i=1}^N (x_i - \mu)^3}{\left(\sqrt{\frac{1}{N} \sum_{i=1}^N (x_i - \mu)^2} \right)^3}.$$

It can help determine whether a nodule contains predominantly high or low intensity pixels.

– *Kurtosis*. Kurtosis measures the sharpness of a peak in the intensity distribution. It is mathematically expressed as:

$$Kurtosis = \frac{\frac{1}{N} \sum_{i=1}^N (x_i - \mu)^4}{\left(\sqrt{\frac{1}{N} \sum_{i=1}^N (x_i - \mu)^2} \right)^4} - 3.$$

• **Shape-based features:**

– *Volume*. Volume of a pulmonary nodule is a direct indicator of its size. At the same time, large volumes often require closer scrutiny for potential malignancy. It is calculated by counting the total number of pixels (or voxels in 3D) that make up a segmented nodule and multiplying by the spatial pitch of the pixel (or voxel) to convert to physical units (e.g., cubic millimeters). The volume V is defined as:

$$V = N \times (d)^3,$$

where N is the number of pixels in a nodule, d is the pixel distance.

– *Surface area*. Surface area gives an indication of the complexity of the nodule's appearance. A more irregular surface area may indicate a higher likelihood of malignancy. The surface area A can be approximately calculated using the «marching cubes» algorithm or similar techniques that triangulate the surface of a segmented nodule:

$$A = \sum_{i=1}^M a_i,$$

where M is the total number of triangles approximating the nodule surface, a_i is the area of the i -th triangle. This approximation provides a quantitative measure of the external complexity of a nodule.

– *Sphericity*. Sphericity assesses how much the shape of a nodule resembles a sphere, which is often used to distinguish between regular and irregular nodules. Sphericity Ψ is defined as:

$$\Psi = \frac{\pi^{\frac{1}{3}} (6V)^{\frac{2}{3}}}{A},$$

where V is the volume, A is the nodule surface area. Sphericity values close to 1 indicate a more spherical shape, while values far from 1 suggest irregular shapes.

– *Compactness*. Compactness measures the density of the nodule shape, indicating how densely packed the structure is. It is inversely proportional to sphericity and can be expressed as:

$$C = \frac{A}{V^{\frac{2}{3}}}.$$

A higher compactness value implies a more irregular or complex nodule shape, which may indicate malignancy.

• **Texture features:**

– *Entropy*. Entropy measures randomness or disorder in the intensity distribution of nodule pixels, serving as an indicator of texture irregularity. High entropy values suggest a complex texture with a high degree of heterogeneity, which is often observed in malignant tumors. Entropy is calculated by the formula:

$$H = -\sum_{i=0}^{L-1} \sum_{j=0}^{L-1} p(i, j) \log_2 p(i, j),$$

where $p(i, j)$ is normalized co-occurrence matrix, representing the probability of neighboring intensity of pixel i next to intensity of pixel j , L is the number of possible intensity levels.

– *Contrast*. The contrast quantifies local variations in pixel intensity, emphasizing the presence of distinct edges or patterns in a nodule. It reflects the depth of the texture and the sharpness of image details. High contrast values are associated with textures containing significant differences between pixel intensities. Contrast is calculated by the formula:

$$C = \sum_{n=0}^{N-1} \left[n^2 \sum_{i, j | |i-j|=n} p(i, j) \right],$$

where N is the number of different intensity levels, n is the difference in intensity levels being considered. This calculation emphasizes the contribution of pixel pairs with significantly different intensities.

– *Homogeneity*. Homogeneity measures the degree of consistency or evenness of the texture. High values of uniformity indicate a smooth, regular texture, while lower values indicate a variety of patterns and irregularities. Homogeneity is defined as:

$$\Gamma = -\sum_{i=0}^{L-1} \sum_{j=0}^{L-1} \frac{p(i, j)}{1 + |i - j|}.$$

This equation weights the elements of the co-occurrence matrix by the inverse of their distance from the diagonal, favoring homogeneous textures where pixel intensities are similar.

– *Correlation*. Correlation estimates the degree of linear dependence between pixel intensities in a given direction within the region of interest. It helps to identify oriented textures and structured patterns. A high correlation indicates a strong relationship between pixel intensity levels across the texture. The correlation is calculated by the formula:

$$\rho = \frac{\sum_{i=0}^{L-1} \sum_{j=0}^{L-1} (i - \mu_i)(j - \mu_j) p(i, j)}{\sigma_i \sigma_j},$$

where μ_i and μ_j are mean values, σ_i and σ_j are standard deviations of the sums of rows and columns of the co-occurrence matrix, respectively. This indicator provides information about the predictability and structure of texture patterns.

Fig. 1 shows a flowchart describing the process of generating, combining and selecting radiomic and deep convolutional features. The radiomics and deep convolution features are combined into a vector, which is fed to the algorithm to select the most important features. Based on the selected features, a new vector is formed which is used to determine the classification of image textures.

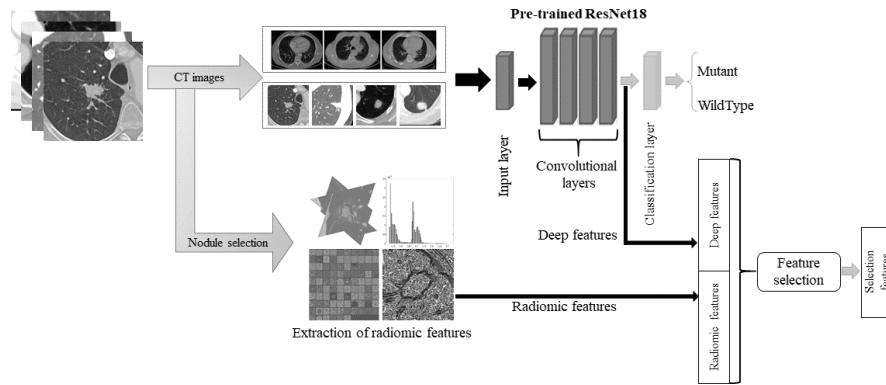


Fig. 1. Flowchart of the proposed method

Features integration

In this paper, a combined approach is applied to analyze radiomic and deep convolutional features using support vector method (SVM) and mRMR (minimum Redundancy Maximum Relevance) feature selection algorithm [9, 10]. These methods play a key role in improving the performance of predictive models by identifying the most significant features that contribute to the determination of the presence of mutations [11].

The mRMR algorithm is used for initial feature selection, minimizing redundancy and maximizing relevance with respect to the target variable. Features that have both maximum correlation with the target variable and minimum correlation with each other are selected for further analysis, thereby improving the informativeness of the data:

$$\max D(S, C) = \frac{1}{|S|} \sum_{x_i \in S} I(x_i; C),$$

where S is selected features set, C is target variable, $I(x_i; C)$ is mutual information between feature x_i and target variable.

Minimum redundancy is defined as minimizing the average mutual information between feature pairs in the selected set:

$$\min R(S) = \frac{1}{|S|^2} \sum_{x_i, x_j \in S} I(x_i; x_j),$$

where $I(x_i; x_j)$ is mutual information between features x_i and x_j .

Combining these two criteria, mRMR algorithm seeks to find the feature set S that optimizes the function:

$$\max \Phi(S) = D(S, C) - R(S),$$

which ensures the selection of features most useful for modeling while minimizing their redundancy. This approach improves the quality of classification, making the model more interpretable and effective in recognizing complex patterns.

The selected features are then analyzed using SVM to assess their ability to classify CT image textures for mutations. This step evaluates how radiomic and deep convolutional features affect model accuracy by providing quantitative performance measures such as *Accuracy*, *Precision* and *Recall*.

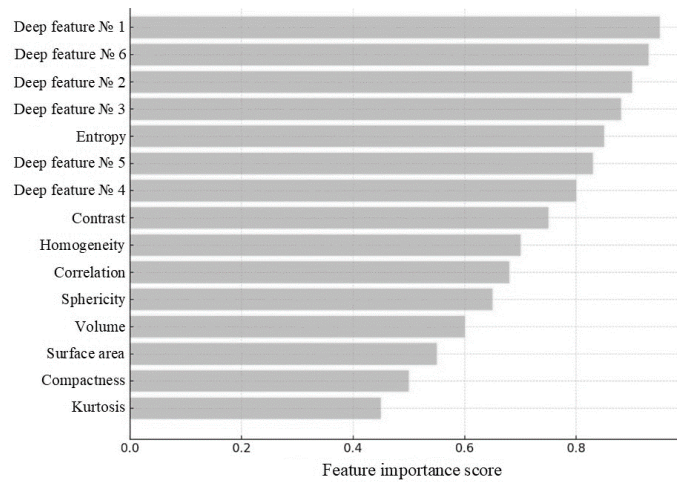


Fig. 2. Assessing the importance of features

This approach not only allows us to compare the performance of radiomic and deep convolutional features, but also to improve our understanding of their interactions and contributions to determining the presence of mutations. This methodology emphasizes the unique contributions of each type of feature and their potential to improve the diagnostic accuracy of models.

Results and discussion

Fig. 2 shows the interaction between traditional radiomic features, such as “Entropy” (0.85), “Contrast” (0.75) and “Sphericity” (0.65) and features obtained by deep learning, including “Deep Feature 1” (0.95) and “Deep Feature 6” (0.93) (the number denotes the position of the selected features in the original vector, with dimensionality 1×512), etc.

The feature importance analysis determined by the mRMR method provides insight into the predictive power of the proposed integrated model for classifying CT image texture for mutations. It can be concluded that deep learning features rank high in importance, emphasizing the depth of information they include about the underlying pathology. However, the significant ranking of radiomic features suggests that they also provide essential, unreliable information useful for the classification task.

Table

Comparison of the effectiveness of approaches for determining the presence of mutations in the EGFR gene

Method	Accuracy, %
Deep convolutional features + SVM	89
Radiomic features + SVM	87
Deep convolutional features + Radiomic features + SVM	92
“Mut-SeResNet” [14]	88

In this study, we compared the efficacy of different approaches to determine the presence of mutations in the EGFR gene using SVM [1, 12, 13]. The results are presented in Table. As can be seen from the table, the model developed and tested in our study showed the highest accuracy among the approaches considered, achieving an Accuracy of 92%. Compared to another study [14] using traditional approaches and specialized models, our approach shows improved results, which may contribute to a more accurate and efficient diagnosis.

Conclusion

The paper considers the problem of comparing and selecting radiomic and deep convolutional features extracted from CT images in order to improve the accuracy of CT image texture classification. Using the mRMR algorithm, the effectiveness of radiomics features in classification tasks was demonstrated. Then, a classifier was developed that showed high accuracy in classifying the presence of genetic mutations among the considered approaches, achieving an Accuracy of 92%. Analysis of the results showed that deep learning features reveal high-level abstract textures indicative of underlying pathologies, while radiomic features provide essential information about tumor phenotypic features such as shape, texture, and intensity.

REFERENCES

1. **Skalunova M., Shariaty F., Rozov S., Radmard A.R.** Personalized Chemotherapy Selection for Lung Cancer Patients Using Machine Learning and Computed Tomography. *International Conference on Electrical Engineering and Photonics (EExPolytech)*, 2023, pp. 128–131. DOI: 10.1109/EExPolytech58658.2023.10318700
2. **Taranova D., Shariaty F.** Radiomic analysis for prediction of T stage parameter (T1–T2) in lung cancer patients. *Proceedings of the All-Russian Conference “Science Week IET”*, 2022, pp. 77–80.
3. **Pavlov V.A., Zavjalov S.V., Pervunina T.M., Orooji M., Shariaty F.** Application of deep learning for COVID-19 classification and pulmonary edema on pulmonary CT images. *Voprosy radioelektroniki. seriya: tekhnika televideniya [Issues of radio electronics. Series: Television technology]*, 2022, no. 1, pp. 65–72.
4. **Zavjalov S.V., Pavlov V.A., Fyodorov S.A., Shariaty F., Pervunina T.M.** Automatic segmentation and classification of COVID-19 on CT images. *Voprosy radioelektroniki. seriya: tekhnika televideniya [Issues of radio electronics. Series: Television technology]*, 2023, no. 4, pp. 76–83.
5. **Bakr S., Gevaert O., Echegaray S. et al.** A radiogenomic dataset of non-small cell lung cancer. *Scientific data*, 2018, Vol. 5, no. 1, Article no. 180202. DOI: 10.1038/sdata.2018.202
6. **Amiri S., Akbarabadi M., Abdolali F., Nikoofar A., Esfahani A.J., Cheraghi S.** Radiomics analysis on CT images for prediction of radiation-induced kidney damage by machine learning models. *Computers in Biology and Medicine*, 2021, Vol. 133, Article no. 104409. DOI: 10.1016/j.compbiomed.2021.104409
7. **Reiazi R., Abbas E., Famiyeh P., Rezaie A., Kwan J.Y.Y., Patel T., Bratman S.V., Tadic T., Liu F.F., Hai-be-Kains B.** The impact of the variation of imaging parameters on the robustness of Computed Tomography radiomic features: A review. *Computers in Biology and Medicine*, 2021, Vol. 133, Article no. 104400. DOI: 10.1016/j.compbiomed.2021.104400
8. **Shiri I., Sorouri M., Geramifar P., Nazari M., Abdollahi M., Salimi Y., Khosravi B., Askari D., Aghaghazvini L., Hajianfar G., Kasaeian A., Abdollahi H., Arabi H., Rahmim A., Radmard A.R., Zaidi H.** Machine learning-based prognostic modeling using clinical data and quantitative radiomic features from chest CT images in COVID-19 patients. *Computers in Biology and Medicine*, 2021, Vol. 132, Article no. 104304. DOI: 10.1016/j.compbiomed.2021.104304
9. **Wang Z. et al.** Segmentalized mRMR features and cost-sensitive ELM with fixed inputs for fault diagnosis of high-speed railway turnouts. *IEEE Transactions on Intelligent Transportation Systems*, 2023, Vol. 24, no. 5, pp. 4975–4987. DOI: 10.1109/TITS.2023.3239636
10. **Lanjewar M.G., Parab J.S., Shaikh A.Y. et al.** CNN with machine learning approaches using ExtraTreesClassifier and MRMR feature selection techniques to detect liver diseases on cloud. *Cluster Computing*, 2023, Vol. 26, no. 6, pp. 3657–3672. DOI: 10.1007/s10586-022-03752-7
11. **Ding C., Peng H.** Minimum redundancy feature selection from microarray gene expression data. *Journal of Bioinformatics and Computational Biology*, 2005, Vol. 3, no. 2, pp. 185–205. DOI: 10.1142/s0219720005001004

12. Pavlov V.A., Shariaty F., Orooji M., Velichko E.N. Application of Deep Learning Techniques for Detection of COVID-19 Using Lung CT Scans: Model Development and Validation. Springer Proceedings in Physics, 2022, Vol. 268, pp. 85–96. DOI: 10.1007/978-3-030-81119-8_9

13. Sun L., Dong Y., Xu S., Feng X., Fan X. Predicting Multi-Gene Mutation Based on Lung Cancer CT Images and Mut-SeResNet. Applied Sciences, 2023, Vol. 13, no. 3, Article no. 1921. DOI: 10.3390/app13031921

INFORMATION ABOUT AUTHORS / СВЕДЕНИЯ ОБ АВТОРАХ

Shariaty Faridoddin

Шариати Фаридоддин

E-mail: shariaty3@gmail.com

ORCID: <https://orcid.org/0000-0002-7060-8826>

Pavlov Vitalii A.

Павлов Виталий Александрович

E-mail: pavlov_va@spbstu.ru

ORCID: <https://orcid.org/0000-0003-0726-6613>

Surakov Murat U.

Сураков Мурат Уралович

E-mail: murat.surakov@gmail.com

Submitted: 15.04.2024; Approved: 06.07.2024; Accepted: 19.07.2024.

Поступила: 15.04.2024; Одобрена: 06.07.2024; Принята: 19.07.2024.